# Corneal Sulfated Glycosaminoglycans and Their Effects on Trigeminal Nerve Growth Cone Behavior In Vitro: Roles for ECM in Cornea Innervation

*Tyler Schwend,*[*,1] *Ryan J. Deaton,*[2] *Yuntao Zhang,*[1] *Bruce Caterson,*[3] *and Gary W. Conrad*[1]

**Purpose.** Sensory trigeminal nerve growth cones innervate the cornea in a highly coordinated fashion. The purpose of this study was to determine if extracellular matrix glycosaminoglycans (ECM–GAGs), including keratan sulfate (KS), dermatan sulfate (DS), and chondroitin sulfate A (CSA) and C (CSC), polymerized in developing eyefronts, may provide guidance cues to nerves during cornea innervation.

**Methods.** Immunostaining using antineuron-specific-β-tubulin and monoclonal antibodies for KS, DS, and CSA/C was performed on eyefronts from embryonic day (E) 9 to E14 and staining visualized by confocal microscopy. Effects of purified GAGs on trigeminal nerve growth cone behavior were tested using in vitro neuronal explant cultures.

**Results.** At E9 to E10, nerves exiting the pericorneal nerve ring grew as tight fascicles, advancing straight toward the corneal stroma. In contrast, upon entering the stroma, nerves bifurcated repeatedly as they extended anteriorly toward the epithelium. KS was localized in the path of trigeminal nerves, whereas DS and CSA/C–rich areas were avoided by growth cones. When E10 trigeminal neurons were cultured on different substrates comprised of purified GAG molecules, their neurite growth cone behavior varied depending on GAG type, concentration, and mode of presentation (immobilized versus soluble). High concentrations of immobilized KS, DS, and CSA/C inhibited neurite growth to varying degrees. Neurites traversing lower, permissive concentrations of immobilized DS and CSA/C displayed increased fasciculation and decreased branching, whereas KS caused decreased fasciculation and increased branching. Enzymatic digestion of sulfated GAGs canceled their effects on trigeminal neurons.

**Conclusions.** Data herein suggest that GAGs may direct the movement of trigeminal nerve growth cones innervating the cornea. (*Invest Ophthalmol Vis Sci.* 2012;53:8118–8137) DOI: 10.1167/iovs.12-10832

The extracellular matrix (ECM) provides regulatory cues that govern growth and guidance of axonal growth cones in the developing peripheral nervous system (PNS). These cues may be growth-promoting, growth-permissive, or growth-inhibitory, dependent on both the nature of the ECM molecule(s) and the context in which they are presented in the peripheral tissue to growth cones. Inhibitory ECM molecules in the PNS serve as barriers to block and steer axonal growth cones from projecting into inappropriate tissues and keep them headed toward their target tissue, whereas simultaneously, growth-promoting factors serve to positively attract growth cones.[1] In this manner, sensorimotor innervation during early PNS development is dependent on transient spatiotemporal distributions of ECM molecules with differential potentials for influencing nerve-growth cone behavior.

Proteoglycans (PGs) represent a class of glycoproteins that carry sulfated polysaccharide side chains and are commonly enriched in nonpermissive peripheral tissues that border the pathways of growing axons during PNS development. PGs are composed of a core protein covalently attached to glycosaminoglycans (GAGs), long unbranched polysaccharide chains of repeating disaccharide units. Each disaccharide unit contains either D-glucuronic acid (GlcA), L-iduronic acid (IdoA), or D-galactose (Gal) paired in each disaccharide with either D-*N*-acetylglucosamine (GlcNAc) or D-*N*-acetylgalactosamine (GalNAc), with one or both of the sugars in each disaccharide sulfated, and thus highly charged ionically (Fig. 1). The adult human corneal stroma contains (by weight) 65% keratan sulfate (KS) and 30% chondroitin/dermatan sulfate (CS or DS),[2] which were each first described as major corneal GAGs by Meyer and colleagues.[3,4]

Chondroitin sulfate proteoglycans (CSPGs) influence many biological functions, including cell adhesion, cell migration, axonal guidance and pathfinding, and axonal fasciculation/defasciculation behavior.[5–7] With respect to axonal growth cone movement, CSPGs in the ECM have been shown to be inhibitory both in vitro[8–22] and in vivo.[23–29] Interestingly, other studies have reported positive effects of CSPGs on neurite outgrowth.[30–33] Differential effects on neuronal growth likely arise from the high degree of polymorphism of PGs and GAGs,[5] their sulfation patterns in ''hot spots'' along GAG chains,[31,34–37] their mode of presentation to neuronal growth cones (i.e., immobilized versus soluble),[38] and their reversible binding and release of growth factors, guidance cues, and other ECM molecules of small and large molecular size and

From the [1]Division of Biology, Kansas State University, Manhattan, Kansas; the [2]Department of Pathology, University of Illinois at Chicago, Chicago, Illinois; and [3]Connective Tissue Biology Laboratories, School of Biosciences, Cardiff University, Cardiff, Wales, United Kingdom.

Supported by an individual Ruth L. Kirschstein Postdoctoral National Research Service Award/National Eye Institute/National Institutes of Health (NEI/NIH) Grant F32 EY021708 (TS), NEI/NIH Grant R01 EY000952 (GWC), funding from the Research Career Development Core (Brychta) in the Division of Biology at Kansas State University GOBO000657 (GWC), and by NIH-P20-RR017686 to the Center of Biomedical Research Excellence Core B in the Veterinary School at Kansas State University. The authors alone are responsible for the content and writing of the paper.

Submitted for publication August 23, 2012; revised October 16, 2012; accepted October 27, 2012.

Disclosure: **T. Schwend**, None; **R.J. Deaton**, None; **Y. Zhang**, None; **B. Caterson**, None; **G.W. Conrad**, None

Current affiliation: *Department of Comparative Biosciences, College of Veterinary Medicine, University of Illinois at Urbana-Champaign, 3411 Vet Med Basic Sciences, Urbana, Illinois.

Corresponding author: Gary W. Conrad, Division of Biology, Ackert Hall, Kansas State University, Manhattan, KS 66506; gwconrad@ksu.edu.



Investigative Ophthalmology & Visual Science, December 2012, Vol. 53, No. 13

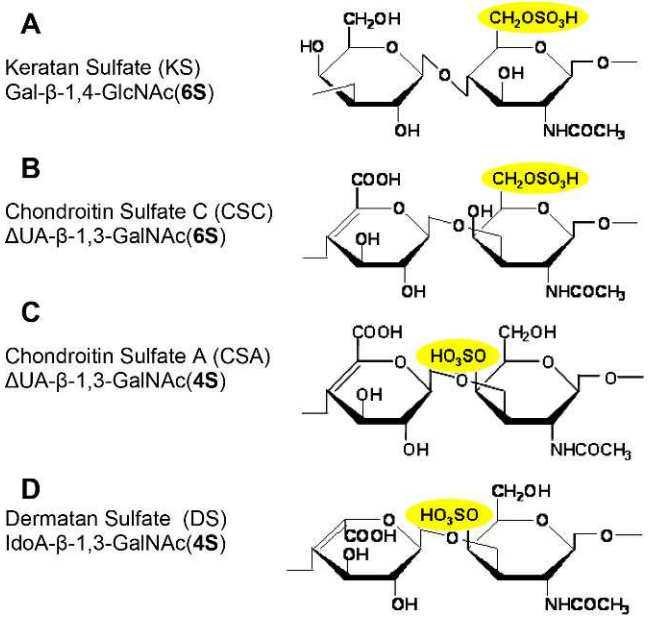


**Figure 1.** Schematic chemical structures of the repeating disaccharide unit of GAGs used in this study. (**A**) KS: $[Gal\text{-}\beta\text{-}1,4\text{-}GlcNAc(6S)]_n$. KS repeating disaccharide unit is composed of alternating residues of D-galactose (Gal) and *N*-acetyl-D-glucosamine (GlcNAc) linked β-1,4 and β-1,3, and hydroxyl groups at the C-6 positions of Gal and GlcNAc residues may be sulfated. (**B**) CSC: $[\Delta UA\text{-}\beta\text{-}1,3\text{-}GalNAc(6S)]_n$. CSC repeating disaccharide unit is composed of *N*-acetylgalactosamine (GalNAc) residues alternating in β-1,3-glycosidic linkages with glucuronic acid (ΔUA) residues, and sulfated primarily at the C-6-position of GalNAc residue. (**C**) CSA: $[\Delta UA\text{-}\beta\text{-}1,3\text{-}GalNAc(4S)]_n$. CSA repeating disaccharide unit is composed of *N*-acetylgalactosamine (GalNAc) residues alternating in β-1,3-glycosidic linkages with glucuronic acid (ΔUA) residues, and sulfated primarily at the C-4-position of GalNAc residues. (**D**) DS: $[IdoA\text{-}\beta\text{-}1,3\text{-}GalNAc(4S)]_n$. DS repeating disaccharide unit is composed of *N*-acetylgalactosamine (GalNAc) residues alternating in β-1,3-glycosidic linkages with iduronic acid (IdoA) residues, and sulfated primarily at the C-4-position of GalNAc residues.

charge.[39–41] Moreover, the developmental context of the cell–ECM interaction, such as the origin and history of the neuron and the presence of other ECM molecules in the substratum, likely also influences the behavior of neuronal growth cones traversing the ECM. Keratan sulfate proteoglycans (KSPGs) also are generally considered to constitute inhibitory barriers to axonal growth.[42–47] Based on findings from many of the above studies, which studied the biological function of the GAG chain independently of the PG core protein, it is now generally believed that the sulfated GAG moiety contributes substantially, if not wholly, to the nerve-influencing function of the CS/KSPGs. In support of this, recent reports indicate that animals treated with chondroitinase ABC, which degrades sulfated CSA/CSC/CSB(DS) GAG chains but leaves PG core proteins intact, display enhanced axonal growth, regeneration, and function following nervous system injury.[24,27,48–53] Moreover, digestion of CS–GAG chains in the notochord[54,55] or head[56] during embryonic development leads to growing sensory and motor axons projecting into tissue locations that normally do not support axon growth.

The cornea is the most densely innervated tissue on the surface of the body.[57] The vast majority of those nerves are sensory,[57,58] derived from neural crest–derived neurons residing in the ophthalmic branch (OpV) of the trigeminal ganglion (TG).[59] Chick cornea innervation from the TG is highly regulated. Beginning at embryonic day (E) 4, TG-derived (trigeminal) growth cones grow directionally toward the cornea, approaching its periphery by E5, yet trigeminal growth cones are then repelled from entering the cornea for several days. Trigeminal nerve bundles encountering the margin of the cornea bifurcate into a dorsal and a ventral stream at the cornea, yet stay close to its edge, as though still positively attracted into the stroma, thus eventually forming a complete pericorneal nerve ring.[60] During later corneal development, at E9 to E10, the cornea becomes permissive to a subset of the trigeminal nerve growth cones that are exclusively of neural crest origin, whereas ectodermal placode–derived trigeminal nerve growth cones remain associated with the pericorneal nerve ring.[59] Axons then send growth cones toward the edge of the corneal stroma from all along the circumference of the nerve ring[61] and extend exclusively into the anterior layers of the developing corneal stroma, navigating steadily toward the corneal epithelium,[62] the outermost cell layer on the surface of the eye. In this manner, growth cones avoid innervating posterior stromal regions and the corneal endothelium, lining the innermost surface of the cornea. Currently, the mechanism(s) controlling these axon guidance decisions remain unclear. Increased levels of sulfated GAGs have been reported coincident with nerves beginning to invade the corneal stoma.[63–67] GAGs localized in different anterior–posterior positions in the corneal stroma during innervation may serve to provide specific positive or negative signals to incoming growth cones. In this manner, corneal GAGs may provide selective barriers to neuronal growth cone extension and guidance to ensure that they are guided toward the outermost surface of the cornea, finally penetrating the basement membrane and extensively bifurcating and branching among the epithelial cells.[68]

Despite the robust presence of GAGs in the developing cornea, their potential in guiding corneal nerve growth cones during innervation has not been studied. Moreover, few studies have considered the effects of individual GAG moieties on sensory outgrowth, nor have the effects of GAGs on sensory neurons of the cornea (i.e., neural crest–derived neurons derived from OpV TG) been investigated to date. In the current study we examined differences in the neurite behavior of trigeminal nerve growth cones when challenged with different GAG molecules that are known to be present in the developing corneal stroma. Among the GAGs that were examined herein are KS and DS, the predominant corneal stroma ECM–GAGs, as well as CSA and CSC that are detectable in the limbal mesenchyme and cornea during development. The distribution of each GAG in the cornea was examined by immunohistochemistry at stages concurrent with trigeminal growth cones projecting from the mesenchyme region containing the limbal nerve ring toward the periphery of the corneal stroma (E9), up to a later stage wherein growth cones have progressed to the center of the cornea and anteriorly into the epithelium (E14). We found the distributions for each GAG to be developmentally regulated. CS/DS was localized between corneal cell layers that were mostly avoided by trigeminal axonal growth cones, whereas KS was more broadly localized throughout the cornea in positions both occupied and unoccupied by axonal growth cones. To examine the potential biological relevance of GAGs in cornea innervation, embryonic trigeminal neurons were cultured with purified substratum-bound, or soluble, CSA, DS, CSC, or KS and neurite outgrowth behaviors were analyzed qualitatively and quantitatively. We show that trigeminal neurites displayed a growth response when they encountered GAG molecules bound to substrate, but not when GAGs were presented in a soluble fashion. High concentrations of substrate-bound KS, DS, and CSA/C inhibited neurite growth to varying degrees, with KS showing the weakest inhibitory potential among the GAGs tested. Moreover, neurites travers-

ing over lower, permissive concentrations of immobilized DS and CSA/C displayed increased fasciculation and decreased branching, whereas neurites that traversed similar KS concentrations were mainly nonfasciculated and displayed a high degree of branching. Collectively, these data implicate corneal ECM–GAGs as being involved in cornea innervation and reveal that each type of GAG triggers a unique set of effects on trigeminal neurite growth cone behavior. Understanding the roles of individual GAGs present in the cornea on neuronal behavior should improve our understanding of axon guidance in the cornea during embryonic development and may shed insight into the general failure of injured axonal stumps to regenerate growth cones capable of penetrating the stroma and epithelium following cornea transplantation/penetrating keratoplasty, trauma, or elective surgeries in adult corneas.

## Methods

### Chick Embryo Husbandry

Fertile White Leghorn chicken eggs (Nelson's Hatchery, Manhattan, KS) were stored at 15°C for up to a week before being transferred to a 38°C humidified poultry incubator on E0 and incubated at 45% humidity for up to 14 days.

### Trigeminal Neuron Preparation

Trigeminal ganglia (TG) were dissected from E10 chick embryos into sterile Howard Ringer's saline solution (7.2 g NaCl, 0.17 g $CaCl_2 \cdot 2H_2O$, 0.37 g KCl in 1 L distilled water, pH 7.3) and the proximal region (containing mostly neural crest–derived neurons[59]) of each ganglion was cut into tissue explants using a tungsten needle (Fine Science Tools, Foster City, CA). Explants were cultured in Dulbecco's modified Eagle's medium (DMEM; Gibco, Carlsbad, CA) supplemented with 10% fetal bovine serum, antibiotics (100 units penicillin, 0.1 mg/mL streptomycin; Sigma, St. Louis, MO), and 25 ng/mL nerve growth factor (NGF; Sigma) to support neurogenesis specifically of the neural crest–derived cells of the trigeminal explants,[69,70] rather than those of the ectodermal-placode–derived neuroblasts that also reside in TG. Trigeminal explants were positioned on prepared tissue chamber slides and incubated at 37°C in a humidified, $CO_2$ incubator for 72 hours. After incubation, neuronal explants were fixed in 4% paraformaldehyde and neuronal growth was visualized by immunostaining.

### Substrate Preparation

Tissue culture chamber slides (one- or two-chambered, Lab-Tek; Thermo Fisher Scientific, Waltham, MA) were coated with poly-D-lysine (PDL; 70,000–150,000 KD, 100 μg/mL in borate buffer, pH 8.4; Sigma) overnight at 4°C, washed three times with water, and stored dry at 4°C for up to 2 weeks prior to use. To perform neurite guidance spot assays in which neurite growth cones extending from trigeminal explants encounter immobilized GAG on an otherwise homogeneous growth-supporting substrate, GAGs were immobilized to the PDL-coated slides by depositing 4-μL drops of five different types of GAGs at varying molar concentrations (0.1–5.0 μM in sterile water). GAGs were allowed to adsorb to the slide surface in a humidified chamber at 37°C for 2 days, then the chamber slides were washed three times with sterile water to remove any unbound GAG chains. Deposited GAGs included CSA (C-8529, from bovine trachea; Sigma), DS (previously known as chondroitin sulfate B; C-3788, from porcine intestinal mucosa; Sigma), CSC (C-4384, from shark cartilage; Sigma), KS (from bovine cornea; Seikagaku Corp., Tokyo, Japan), or heparin (H-3393, from porcine intestinal mucosa; Sigma). Water spots served as a control. The exact positions of the control and test spots were outlined on the bottom of the chamber slide using a permanent marker. Prior to adding trigeminal explants, the entire surface of the chamber slide, including the GAG spots and control spots, was further coated with laminin (25 μg/mL in water; Sigma) for 3 hours at room temperature, resulting in a homogeneous layer of laminin on the slide, covering both GAG-bound and GAG-free regions. At the onset of the study we prepared additional substrates, where laminin and GAG solution were mixed together and allowed to adhere to the PDL surface simultaneously, followed by whole-slide coating with laminin. This latter substrate preparation was performed to ensure that changes in neurite growth cone behavior at the GAG spot interface was not simply due to less available binding spots for laminin to PDL following GAG adsorption. Neurite behavior in control and test conditions did not vary between the two different substrate preparations described above; thus, data presented herein are from GAG solutions deposited alone as isolated drops allowed to adhere to PDL, followed by coating the entire culture surface with laminin.

### Soluble GAG Assay

For growth on laminin substrates, tissue culture chamber slides (four-chambered, Lab-Tek; Thermo Fisher Scientific) were coated with PDL and laminin as described above. CSA/C, DS, KS, or heparin was reconstituted in NGF-containing DMEM culture media in a final volume of 0.5 mL at final GAG molarities ranging between 5 and 20 μM. GAG-containing media were added to chamber slides along with trigeminal explants, which were then incubated at 37°C in a humidified, $CO_2$ incubator for 48 hours. For growth in 3-dimensional collagen matrices, neuronal explants first were suspended in soluble collagen solution[69,71,72] that had been mixed with GAGs to generate final GAG molarities ranging between 5 and 20 μM. After orienting the tissues in the collagen solutions, the collagen was allowed to solidify at 37°C under sterile conditions prior to addition of NGF-containing media on top of such gels. After incubation at 37°C in a humidified, $CO_2$ incubator for 48 hours, neuronal explants were fixed in 4% paraformaldehyde and neuronal growth was visualized by immunostaining.

### Enzymatic Digestion of GAG Chains

In some experiments, GAG spots on chamber slides were pretreated with enzyme solutions prior to serving as substrates for trigeminal neurons. Chondroitinase ABC (chABC, from *Proteus vulgaris*, protease free, EC 4.2.2.4; Sigma) was used at 1 mU/mL, pH 8.0, in 0.1 M ammonium acetate buffer to cleave CSA, CSC, and DS while leaving other GAGs unaltered.[67,73] Keratanase II (from *Bacilus* sp.; Seikagaku America, Falmouth, MA) was used at 0.5 mU/mL, pH 6.0, in 0.1 M ammonium acetate buffer to digest KS at sites of sulfated *N*-acetylglucosamine moieties,[67,74] while leaving other GAGs unaltered. Enzyme treatments were carried out overnight in a humidified chamber at 37°C. In control experiments, GAG spots were treated in a similar fashion with enzyme-free ammonium acetate buffer.

### Immunostaining

Nerves were visualized in (1) fixed whole-mount anterior eyefronts, comprised of the cornea and surrounding limbus and sclera tissues that were freed from the adherent lens, iris, retina, and more posterior eye structures; and in (2) fixed trigeminal neuronal explants in culture with antineuronal β-tubulin–specific antibody[75–77] (Tuj1; R&D Systems, Minneapolis, MN) used at a 1:100 dilution in antibody block solution (PBS, 8 g/L NaCl, 0.2 g/L KCl, 1.44 g/L $Na_2HPO_4$, 0.24 g/L $KH_2PO_4$, pH 7.2 [PBS], containing 10% goat serum, 1% bovine serum albumin [BSA], 0.1% Triton X-100), either for 48 hours, when staining nerves in whole-mount tissues, or overnight, when staining trigeminal neuronal explants or dissociated trigeminal neurons, with all staining occurring at 4°C with mild rocking. Fixation was carried out in 4% paraformaldehyde, overnight at 4°C with mild agitation for whole anterior eyefronts and for 1 to 2 hours at room temperature with mild rocking for trigeminal explants in culture. Following three washes in PBS-T (PBS with 0.1% Triton X-100), tissue was incubated for 2 to 3 hours at

room temperature in AlexaFluor 488–labeled goat anti-mouse $IgG_{2a}$ antibody (Molecular Probes, Carlsbad, CA) used at a 1:200 dilution in antibody block solution. For whole-mount corneas from chicks older than E10, corneas were slit radially through the peripheral two thirds of the tissue at three sites around the cornea to allow antibodies to diffuse laterally into the corneal stroma.[78] To visualize the stromal anterior–posterior nerve positions in corneas, Tuj1-stained whole-mount anterior eyefronts were washed twice in PBS-T, then cryoprotected by incubation in increasing concentrations of sucrose (5%–15%) for 3 hours at each concentration at 4°C then added to warmed gelatin solution, which was allowed to form a gel at room temperature to immobilize the cornea in a vertical position. Gelatin-embedded corneas were quick-frozen in dry ice–chilled methanol and frozen to cryostat chucks in optimal cutting temperature compound and sectioned perpendicularly to the anterior–posterior axis at 20 μm with a cryostat (OTF; Hacker-Bright, Fairfield, NJ) at −20°C. Sections were mounted on specially treated slides (Fisherbrand Superfrost Plus slides; Fisher Scientific, Pittsburgh, PA), washed in 37°C PBS for 10 minutes, and mounted in an aqueous low viscosity mounting medium (EMS Shield Mount; Electron Microscopy Sciences, Hatfield, PA) under a coverslip.

To visualize locations of sulfated GAGs in corneas and surrounding tissue, fixed eyefronts were dehydrated through an increasing ethanol series to 100% (v/v), rinsed twice in xylenes, and embedded in paraffin. Paraffin sections of 8 μm were mounted on specially treated slides (Fisherbrand Superfrost Plus slides), dried overnight at 40°C, and stored prior to use in a dessicated box at −20°C. Sections were dewaxed with xylenes and rehydrated in decreasing ethanol series on the day of immunostaining. Rehydrated sections were washed three times in PBS-T and blocked for 30 minutes in 5% goat serum, 1% BSA, 0.1% Triton X-100, then incubated at 4°C overnight in one of the following primary monoclonal antibodies (mAb): mAb CS56 (Sigma) to CSA/C[79,80] (used diluted 1:25 in 1% BSA in PBS-T), mAb I22 (Developmental Studies Hybridoma Bank, University of Iowa, Iowa City, IA) to KS[63,81] (used diluted 1:9 in 1% BST in PBS-T), mAb 7D4 to CSA/C and DS[82–84] (used undiluted), and mAb 5D4 to KS[85] (used diluted 1:2000 in 1% BSA in PBS-T). Following three washes in PBS-T, tissue was incubated in AlexaFluor 488–conjugated goat anti-mouse $IgG_{2a}$, goat anti-rabbit IgG antibody, goat anti-mouse IgG antibody (Molecular Probes), or goat anti-mouse IgG Fab fragments conjugated to FITC (Sigma) used at a 1:200 dilution in antibody block solution. Following antibody staining on cornea sections, nuclei were visualized with a 30-minute incubation in DAPI (Lonza, Allendale, NJ) diluted 1:100 in PBS, washed thrice in PBS, and covered with an aqueous low viscosity mounting medium (EMS Shield Mount) and a coverslip.

## Image Acquisition

Following neuronal culture and staining, images were captured using an epifluorescence stereomicroscope (Leica MZ16F; Leica Microsystems GmbH, Wetzlar, Germany), equipped with a digital camera (Leica DFC 320; Leica Microsystems GmbH). The same microscope and camera also were used for capturing epifluorescence images of whole-mounts and of some sections. Additionally, a confocal microscope (Zeiss LSM 700; Carl Zeiss AG, Oberkochen, Germany) was used to acquire high-magnification *Z*-stack images of stained cornea sections. Confocal projections were generated using commercial software (Zeiss Zen 2010; Carl Zeiss AG).

## Quantification of Neurite Inhibition, Fasciculation, and Outgrowth

To quantify the preferences of neurite processes and their fasciculation behavior as they encountered the GAG substrate in neurite guidance spot assays, trigeminal neuronal explants cultured for 3 days were fixed, stained, and imaged at a magnification (×5, Leica MZ16F; Leica Microsystems GmbH) so that the GAG spot border ran vertically in the center of the image and 1-mm areas of neurite growth were visible on both sides of the spot border. Only neurites from explants that had adhered to GAG-free substrate prior to their processes encountering GAG-bound substrate were scored. The FITC channel was saved as red-green-blue tiff images. The left-hand side of the image represented the control condition, whereas the right-hand side was the test condition. Images were analyzed with a macro designed specifically for this investigation (ImageJ software version 1.45s; developed by Wayne Rasband, National Institutes of Health, Bethesda, MD, http://rsbweb.nih.gov/ij/download.html). The ImageJ macro used and details of its usage are included in a Supplementary File and Supplementary Figure S1 (see Supplementary Material and Supplementary Fig. S1, http://www.iovs.org/lookup/suppl/doi:10.1167/iovs.12-10832/-/DCSupplemental).

Briefly, each image is loaded and then converted to 8-bit grayscale. Next, background subtraction using the rolling ball method with a radius of 50 is conducted. The grayscale image is then bisected and each half is processed separately. An appropriate threshold for neurites versus background was empirically set. The same threshold then was used on all images. The area occupied by neurites and area occupied by background is collected for each image half (control [ControlCond%] and test conditions [TestCond%]) and is expressed as a percentage. The final measure used is the test condition as a percentage of control: (TestCond%/ControlCond%) × 100.

For example, if the control condition is 75% covered with neurites and the test condition is 10% covered with neurites, the measure is: (10/75) × 100 = 13.3% of control.

To score fasciculation and branching behavior of neurite processes extending on intermediate (permissive) concentrations of immobilized GAG substrates, previously described methods for image capture and data analysis were used.[6,86,87] High-magnification images (×10, Leica MZ16F; Leica Microsystems GmbH) were oriented so that the GAG spot border ran vertically near the left-hand side of the image, allowing the subpopulation of neurites extending onto the GAG spot to be clearly visualized in the image field. Only neurite processes extending 300 μm or more onto the GAG or control substrata were scored, or neurites that had branched from these processes that were at least 300 μm in length. Using Fiji-ImageJ software (National Institutes of Health), the width of each neurite (or neurite fascicle bundle) was measured and the numbers of branch points/defasciculation points along each measured neurite were counted.

To quantify neurite outgrowth, previously described methods were applied.[20] Briefly, trigeminal explants cultured for 2 days were fixed, stained, and imaged so that the explant was situated in the center of the image and all processes were visible. Images were analyzed using the simple neurite tracer plug-in for Fiji-ImageJ (National Institutes of Health). Neurite length was traced from the edge of the explant, along the neurite to its growth cone. Neurite length was measured only from trigeminal explants whose growth resembled a halo, with projections in all directions, and whose growth in each direction along the halo was relatively uniform. For each trigeminal explant, 8 to 10 of the longest neurites were identified and measured to derive a mean length of the longest neurites and used to compare neurite lengths between media alone and media containing the various GAGs in solution examined in this study.

# Results

## Distribution of GAGs in the Embryonic Chick Cornea during Early Stages of Cornea Innervation

Trigeminal nerve axon fascicles extending from the OpV of the TG reach the ventrotemporal pericorneal mesenchyme by E5. At this time, trigeminal axons are inhibited from entering the cornea by lens- and corneal-derived repellants Slit and Semaphorin3A.[69,72] Consequently, the main axonal nerve trunks remain deep in the limbal mesenchyme for several days. During this period, trigeminal nerves are not halted by

the lens and corneal nerve guidance repellants, but instead they extend dorsally and ventrally around the cornea periphery into two approximately equal-sized bundles of nerve fibers to form a complete pericorneal nerve ring by E9 (Fig. 2A[62,68,69,72]). To provide observations of cornea innervation at embryonic ages of E9 and older, nerves were visualized in dissected eyefronts by staining with the antineuronal-β-tubulin–specific antibody (Tuj1). Beginning at E9, nerve fibers extended in a tight bundle/fascicle from the nerve ring and advanced through the limbal mesenchyme, in a straight path without branching (arrows), and projected into the corneal stroma (Figs. 2A, 2B; curved dotted line in Fig. 2B denotes the periphery of the cornea, with the cornea positioned at the top of the image and limbus at the bottom of the image). Transverse sections through the E9 eyefront revealed that nerve bundles in the pericorneal nerve ring were positioned all around the cornea, deep in the posterior limbal mesenchyme (Fig. 2C). Furthermore, nerves extending from the nerve ring projected directly and exclusively to the corneal stroma, avoiding the anterior limbal mesenchyme and limbal epithelium (Fig. 2C). By E10, nerve trunks that had projected into the stroma displayed complex branching/bifurcation patterns (open arrowheads), whereas trunk regions of the same nerves lying in the pericorneal limbal mesenchyme appeared thickened and remained unbranched (arrows) (Figs. 2D, 2E). This indicates that the branching/bifurcation behavior of nerves was correlated with where the nerve is localized in the eyefront (limbus versus corneal stroma). Within the stroma, branch points were evident along the trunk, as well as near the advancing growth cones as they progressed toward the epithelium and the center of the cornea (Fig. 2F). Moreover, cornea sections at this stage revealed that corneal nerve fibers and their branches lay exclusively in the anterior stroma, avoiding posterior corneal stroma and endothelium (Fig. 2F), consistent with previous reports by our group and others.[62,68] By E11, corneal nerves had progressed deeper into the cornea and had undergone extensive branching/bifurcation (open arrowheads), resulting in an increase in overall density of the nerve network in the cornea (Figs. 2G, 2H). At this stage, nerve fibers began to penetrate Bowman's layer and the epithelial basement membrane, and nerve growth cones intermingled with the epithelial cells (Fig. 2I). By E12, nerves continued to advance toward the center of the cornea (Figs. 2J, 2K), with the nerve trunks persisting in anterior stroma and the termini of most nerves that had branched from the main trunk residing anterior to Bowman's layer in the epithelium (Fig. 2L; asterisks denote nerve advancement to the epithelium). By E14, nerve fibers that had extended from all along the circumference of the nerve ring had advanced to the corneal center and their terminii covered the entire corneal surface (Figs. 2M, 2N). The dense nerve network continued to reside exclusively in the anterior stoma and epithelial layers of the corneal center, leaving the posterior corneal layers free of peripheral nerve trunks and terminii (Fig. 2O), observations that were also confirmed at later stages (E16; data not shown). In full, observations of cornea innervation between E9 and E14 raised the following questions: (1) What factor(s) regulate the path taken by nerves as they exit the pericorneal nerve ring and traverse exclusively through the limbal mesenchyme and into the anterior stroma en route to the outer epithelial surface of the cornea, leaving the limbal epithelium and posterior corneal stroma and corneal endothelium free of nerves? and (2) What factor(s) determine the different nerve behaviors (i.e., branching/bifurcation) in growing nerves when they are advancing through the limbus tissues (unbranched/fasciculated) versus when they are growing through the corneal stroma and epithelium (high degree of branching/highly nonfasciculated)?

Nerve guidance behaviors throughout the developing embryo have been shown to be regulated by ECM molecules in multiple reports. We therefore sought to examine distributions of ECM–GAG molecules in eyefronts during specific stages during cornea innervation. To do so, the localization patterns of CSA/C, DS, and KS were examined by confocal microscopy in eyefronts following staining with mAb CS56 to CSA/CSC, mAb 7D4 to native CS/DS, and mAbs I22 and 5D4 to KS (see Table 1 for further information on antibodies used in this study). Confocal stack projections of Tuj1 staining in chick eyefronts were also prepared and are provided in Figure 3 to show the progression of nerve growth cones during eye development (Figs. 3A, 3F, 3K, 3P, 3U) alongside the localization patterns for each GAG. At E9, staining with CS-56 (CSA/C) and 7D4 (CS/DS) were present throughout the anterior limbal mesenchyme, but were noticeably absent in the posterior limbal mesenchyme where the nerve ring and nerve fibers were located (Figs. 3A–C). Additionally, staining patterns for 7D4 (CS/DS) were detectable within the corneal stroma; however, staining was absent from the anterior corneal stromal layers that are the direct paths of incoming nerve fibers (Fig. 3C, showing staining in corneal edge; see Supplementary Material and Supplementary Fig. S2, http://www.iovs.org/lookup/suppl/doi:10.1167/iovs.12-10832/-/DCSupplemental, showing staining in the central cornea). It is likely that 7D4 cornea staining in the E9 cornea represents DS epitopes, because CS-56 (CSA/C, but not DS) was absent from the cornea at this stage (Fig. 3B, corneal edge; see Supplementary Material and Supplementary Fig. S2, http://www.iovs.org/lookup/suppl/doi:10.1167/iovs.12-10832/-/DCSupplemental, central cornea). Antibody staining with I22 and 5D4 (both KS) at E9 could not be detected in limbal tissue, yet both KS antibodies stained tissue prominently throughout the corneal stroma, directly in the path of corneal nerves (Figs. 3D, 3E, corneal edge; see Supplementary Material and Supplementary Fig. S2, http://www.iovs.org/lookup/suppl/doi:10.1167/iovs.12-10832/-/DCSupplemental, central cornea). By E10, nerves had traversed through the limbus and their advancing growth cones were now in the anterior stroma (Fig. 3F). Consistent with observations reported above, nerves began to display branching/bifurcation patterns along areas of their trunks located within the corneal stroma (Fig. 3F, open arrowhead). In comparison, CS-56 staining (CSA/C) at E10 was expanded in eyefronts compared with a day earlier, becoming localized throughout the entire limbus and also detectable in the posterior stromal layers of the cornea (Fig. 3G, corneal edge; see Supplementary Material and Supplementary Fig. S2, http://www.iovs.org/lookup/suppl/doi:10.1167/iovs.12-10832/-/DCSupplemental, central cornea). At this stage, the staining pattern for CS-56 (CSA/C) in the cornea was localized to similar regions as 7D4 staining (CS/DS) and both staining patterns were noticeably absent in the anterior stroma, where nerves were detected (Figs. 3G, 3H). In contrast, staining patterns with I22 and 5D4 (both to KS) remained absent in the limbus yet were detectable within all corneal layers at E10 (Figs. 3I, 3J, corneal edge; see Supplementary Material and Supplementary Fig. S2, http://www.iovs.org/lookup/suppl/doi:10.1167/iovs.12-0832/-/DCSupplemental, central cornea). At E11, nerves continued to progress through the anterior stroma, toward the epithelial layer (Fig. 3K), whereas the staining patterns for CS-56 (CSA/C) and 7D4 (CS/DS) remained localized to limbal tissues (data not shown) and to corneal stroma layers that were directly posterior to nerves (Figs. 3L, 3M). Meanwhile, I22 and 5D4 staining (both to KS) persisted throughout all stromal layers, regardless of the absence or the presence of nerves (Figs. 3N, 3O). At E12 to E14, time points when advancing nerve growth cones have progressed into the corneal epithelium (Figs. 3P, 3U), CS-56 (CSA/C), and 7D4 (CS/DS)

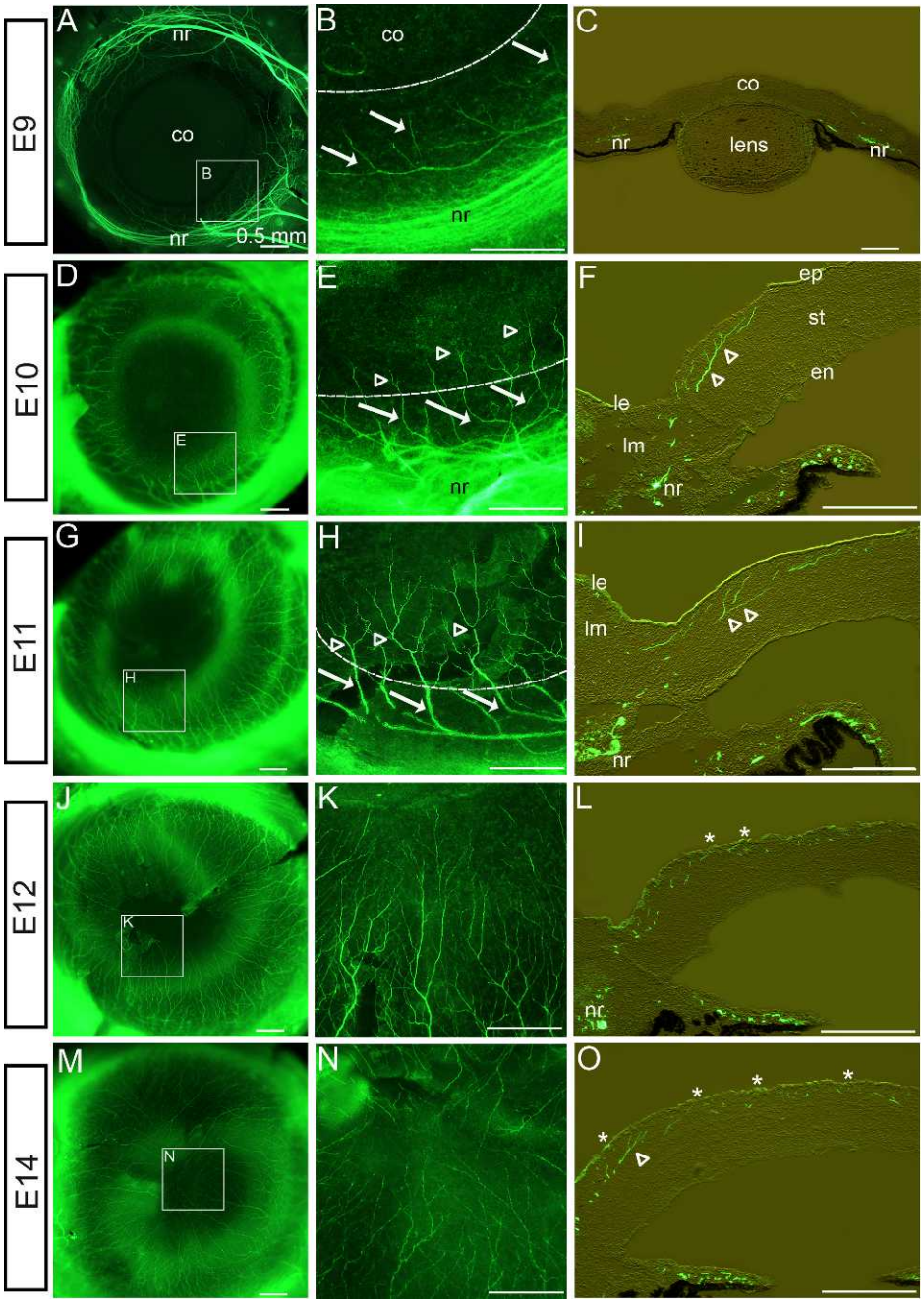


**Figure 2.** Cornea innervation by trigeminal sensory nerves during development. (**A–C**) Nerves visualized in cornea whole-mounts (**A**, **B**) or sections (**C**) at E9 following staining with antineuronal β-tubulin-specific Tuj1 antibody, detected with AlexaFluor 488 (*green*), could be seen having grown around the cornea in the limbus, forming a pericorneal nerve ring. At this stage, individual nerves or nerve bundles/fascicles exited the nerve ring and advanced in a straight path, without branching (*arrows* in [**B**] show individual nerves), to the cornea. *Dotted, curved line* denotes corneal periphery. (**D–I**) At E10 to E11, nerves that had penetrated the cornea began to branch/bifurcate ([**E**, **F**, **H**, **I**] *open arrowheads* show branch points) along their trunks and advancing terminii, whereas nerve trunks within the limbus remained unbranched ([**E**, **H**] *solid arrows*). Nerves in the cornea advanced exclusively within the anterior stroma, avoiding the posterior stroma and endothelium (**F**, **I**). (**J–O**) Between E12 and E14, nerves continued to advance to the cornea's center (**J**), eventually reaching it by E14 (**M**). Increased branching along the corneal-lying nerve trunks increased the overall density of the neural network in the cornea (**K**, **N**). By E12, nerve growth cones had advanced anteriorly to penetrate among the epithelial cells (*asterisks*, [**L**, **O**]). Despite the extensive innervation of the chick eyefront during these stages, nerve staining never became visible in the limbal epithelium, the anterior limbal mesenchyme, or the posterior cornea layers. *Scale bar*, 0.5 mm. en, corneal endothelium; ep, corneal epithelium; co, cornea; nr, nerve ring; le, limbal epithelium; lm, limbal mesenchyme; st, corneal stroma.

staining appeared to expand into more posterior corneal layers, but staining for each antibody remained absent in the anterior stroma (Figs. 3Q, 3R, 3V, 3W). Moreover, at these stages, CS-56 (CSA/C) and 7D4 (CS/DS) staining was much more robust in the limbus, compared with the corneal tissues, indicating a rise in the levels of CS and DS epitopes in the limbus between E9 and E14 (Figs. 4B, 4C). At concurrent stages, I22 and 5D4 staining (both for KS) continued to persist throughout all corneal stromal layers (Figs. 3S, 3T, 3X, 3Y), and was absent in the limbus (Figs. 4D, 4E).

**Table 1.** Monoclonal Antibodies Used in This Study

| mAb Name | Antigen | References |
|---|---|---|
| Tuj1 | Neuron-specific class III β-tubulin | 75 to 77 |
| 5D4 | Highly sulfated KS sulfate domains | 85 |
| I22 | Cornea and cartilage KS sulfate domains | 63, 81 |
| 7D4 | CS/DS sulfate domains (CSA/C, DS) | 82 to 84 |
| CS-56 | CS sulfate domains (CSA/C) | 79, 80 |

In full, evidence obtained from investigating CS-56 (CSA/C) and 7D4 (CS/DS) staining during E9 to E14 revealed that the epitopes for CSA/C and DS were localized in similar regions of pericorneal and corneal tissues and could be found consistently in eyefront tissues which developing nerves avoided, suggesting that nerves projecting from the pericorneal nerve ring through the limbus and into the cornea are restricted from growing into eyefront areas containing high amounts of CS and DS molecules. In contrast, during E9 to E14 the KS epitopes in the eyefronts were found exclusively in the corneal stroma, in all layers, including corneal layers that developing nerves traverse. The KS localization patterns during stages of cornea innervation do not suggest that its presence restricts nerve projections; however, nerve branching occurred exclusively in eyefront tissues where KS was localized, indicating that KS may regulate nerve behavior, specifically in triggering branching/defasciculation. Collectively, the corneal ECM staining patterns reported here raised the intriguing hypothesis that ECM–GAGs

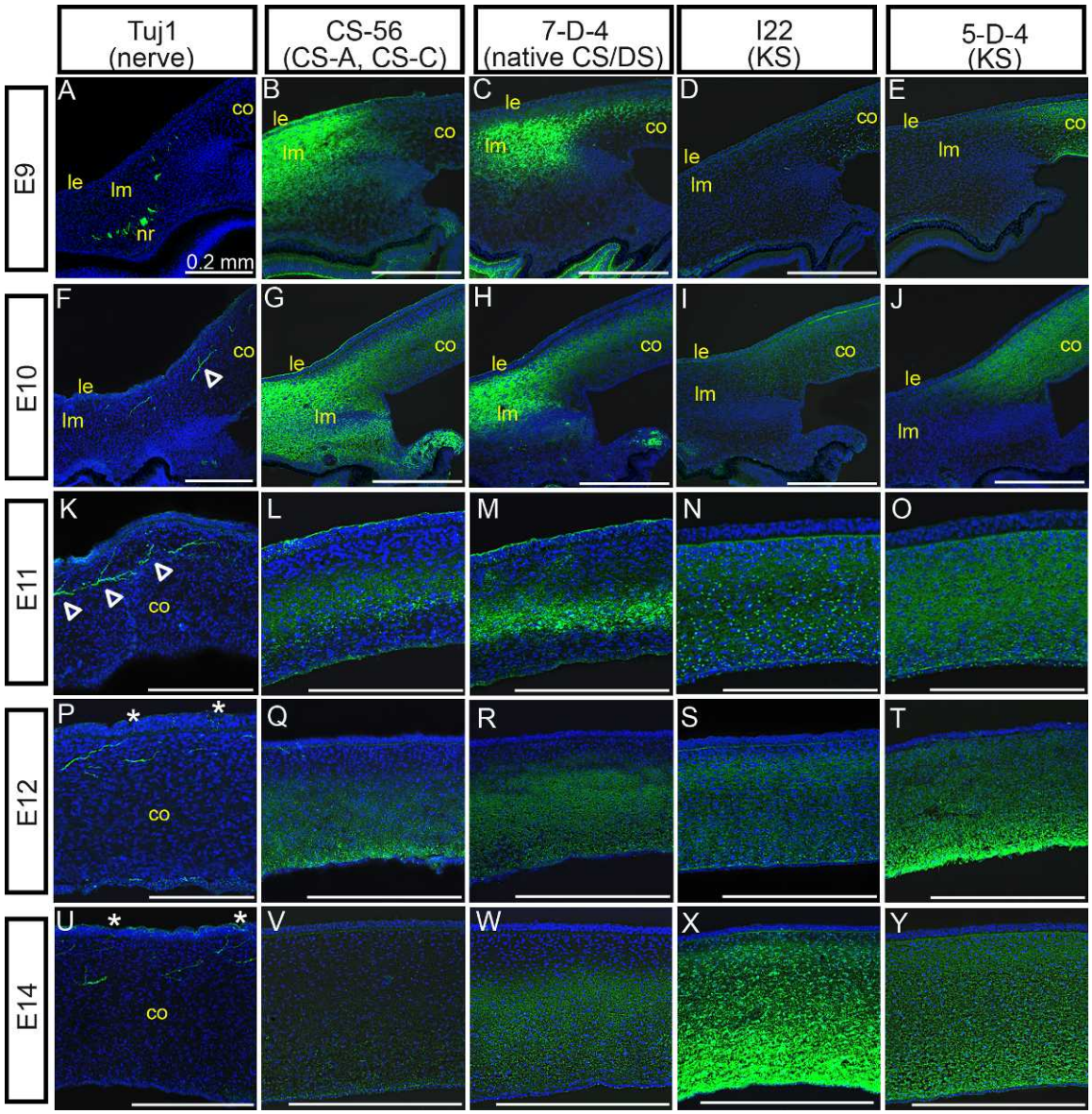


**Figure 3.** GAG distributions in corneal and pericorneal tissues during innervation. Position of corneal nerves compared to distribution of sulfated GAGs in developing eyefronts within confocal stack projections following staining with monoclonal antibodies neuronal-specific Tuj1 (**A**, **F**, **K**, **P**, **U**), CS-56 for CSA/C (**B**, **G**, **L**, **Q**, **V**), 7D4 for CS/DS (**C**, **H**, **M**, **R**, **W**), I22 for KS (**D**, **I**, **N**, **S**, **X**), and 5D4 also for KS (**E**, **J**, **O**, **T**, **Y**), detected with AlexaFluor 488– or FITC-labeled secondary antibodies (*green*) at E9 ([**A–E**]; images show staining in pericorneal tissue and corneal edge), E10 ([**F–J**]; images show staining in corneal edge), E11 ([**K–O**]; images show staining in mid-central cornea), E12 ([**P–T**]; images show staining in central cornea), and E14 ([**U–Y**]; images show staining in central cornea) days of incubation. Cell nuclei are stained *blue* with DAPI. *Open arrowheads* in (**F**, **K**) delineate branching from main nerve trunk. *Asterisks* in (**P**, **U**) denote positive nerve staining in the epithelial layer of the cornea. *Scale bars*, 0.2 mm. co, cornea; nr, nerve ring; le, limbal epithelium; lm, limbal mesenchyme.

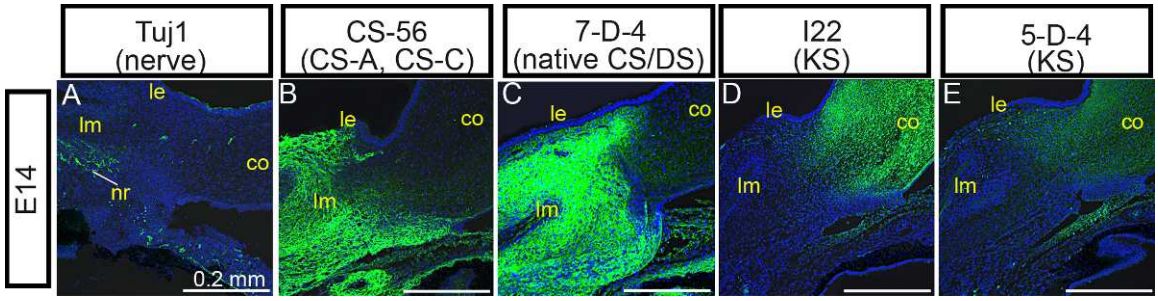


**Figure 4.** GAG distribution in pericorneal tissues at E14. Position of pericorneal nerve ring compared with distribution of sulfated GAGs in the pericorneal tissue within confocal stack projections following staining with monoclonal antibodies neuronal-specific Tuj1 (**A**), CS-56 for CSA/C (**B**), 7D4 for CS/DS (**C**), I22 for KS (**D**), and 5D4 also for KS (**E**), detected with AlexaFluor 488– or FITC-labeled secondary antibodies (*green*) at E14 days of incubation. Cell nuclei are stained *blue* with DAPI. *Scale bars*, 0.2 mm. co, cornea; nr, nerve ring; le, limbal epithelium; lm, limbal mesenchyme.

may influence sensory innervation of the cornea, which provided the rationale for the following in vitro functional studies that were chosen for this investigation.

## CS, DS, and KS GAGs Are Potent Inhibitors of Trigeminal Neurite Outgrowth In Vitro

To examine the possibility that GAGs present in the embryonic limbus and cornea may guide and direct trigeminal growth cones during pathfinding from the pericorneal nerve ring to the corneal epithelium, we used an in vitro axonal spot guidance assay[88] designed to present immobilized GAGs in combination with both PDL and laminin to growth cones as they extend from trigeminal explants. To achieve this, 4 μL of purified CSA, CSC, DS, or KS in water was spotted on PDL-coated glass surfaces and left to bind to PDL over the course of 2 days in a humidified, 37°C tissue culture incubator. Next, unbound GAGs were removed by water washes and then the entire culture surface was coated with laminin to promote neuronal attachment,[8] leaving a small, circular GAG spot for neuronal growth cones to ignore, avoid upon initial contact, or spread upon avidly (see Supplementary Material and Supplementary Fig. S3, http://www.iovs.org/lookup/suppl/doi:10.1167/iovs.12-10832/-/DCSupplemental) among a uniform PDL/laminin substrate. To present GAGs only to growth cones, not to the cell bodies, as the nerves would encounter these varying substrates in the embryo normally in vivo, explants derived from the proximal half of the OpV of E10 TG were seeded on the PDL/LN (GAG-free) surface adjacent to the GAG spot boundary, thus allowing the outgrowing growth cones one sector in which to encounter the GAG spot and then to reveal their decisions about whether to migrate upon it or avoid it (Fig. 5A). At high concentrations of CSA and CSC or DS, most neurite growth cones were deflected at the border of the spot and did not cross over the GAG surface (Figs. 5D, 5F, 5H; GAG spot is denoted in images by white, dotted circular line). In comparison, neither a control spot of water nor a spot made of an equal molar concentration of heparin (Hep), the most sulfated GAG in nature, inhibited neurite advancement at the spot interface, given that neurites extended freely onto these substrates (Figs. 5B, 5C). These findings indicated that neither steric hindrance nor negatively charged substrata could be considered a significant factor in governing the growth cone choice between extending onto GAG-free substrate or onto substrate-containing GAG in our assay. The inhibitory activity of CSA/C and DS spots on neurites was reduced, but not completely removed, when the chondroitin and dermatan sulfate chains were digested by treatment with chondroitinase ABC (chABC) (Figs. 5E, 5G, 5I). Loss of GAG chains on the culture surface following chABC treatment was confirmed by a loss in fluorescent intensity following antibody staining (see Supplementary Material and Supplementary Fig. S3, http://www.iovs.org/lookup/suppl/doi:10.1167/iovs.12-10832/-/DCSupplemental). This indicated that the inhibitory effect of CS and DS on the migratory behavior of neurite growth cones in this assay is due to the GAG chain domains and not due to short peptides of core proteoglycans still attached to the reducing end of GAG chains.

In comparison with CSA/C and DS molecules, immobilized KS was not as effective at inhibiting trigeminal neurite growth cone migration when spotted at an equal molar concentration (Fig. 5J). Although many neurite growth cones were inhibited at the KS spot boundary, not all were repelled and some extended freely onto the KS-bound substrate (Fig. 5J, arrows). Digestion of the KS moieties by keratanase (KSase) II allowed a much higher percentage of neurites to traverse the KS spot (Fig. 5K), indicating that sulfated KS chains were the source of the mild inhibitory effect on trigeminal neuronal growth cones.

Since CS and DS GAGs displayed equal potency of inhibition on trigeminal neurites at high levels, we performed dose–response assays to determine their differing potentials to inhibit axonal crossing at lower concentrations. To clearly visualize neurite growth at the border between the GAG spot and GAG-free substrate, high-magnification images were captured to include nerve growth on both GAG-free and GAG-containing substrates, with the boundary between the different substrates lying at the image center (indicated by vertical dotted lines in Fig. 6). Qualitatively, it was apparent that decreasing the concentrations of CSA/C, DS, or KS used in the assay allowed significantly increased numbers of neurite growth cones to migrate over the respective immobilized GAG spots (Figs. 6A–I). A decreasing concentration of CS–GAG immobilized to the PDL substrate was visualized by decreasing fluorescent intensity upon CS56 immunostaining (see Supplementary Materials and Supplementary Fig. S3, http://www.iovs.org/lookup/suppl/doi:10.1167/iovs.12-10832/-/DCSupplemental).

To quantify the difference in neurite behavior upon encountering varying concentrations of immobilized GAGs, we designed a macro-based software program to be used in this assay, which compared the neuritic density on each side of the boundary between GAG-free and GAG-containing substrates, allowing us to measure changes in neuronal outgrowth as neurites encounter differences in substrate (details of the macro are described in the Methods section and Supplementary Fig. S1; the macro is included as a Supplementary File; see Supplementary Material and Supplementary Fig. S1, http://www.iovs.org/lookup/suppl/doi:10.1167/iovs.12-10832/-/DCSupplemental). To do this, neurite density was recorded on each side of the boundary using NIH-ImageJ software. For each image, neurite density levels on the GAG-free side of the boundary were normalized to a value of 100% neurite density and a corresponding percentage for neurite density, relative to

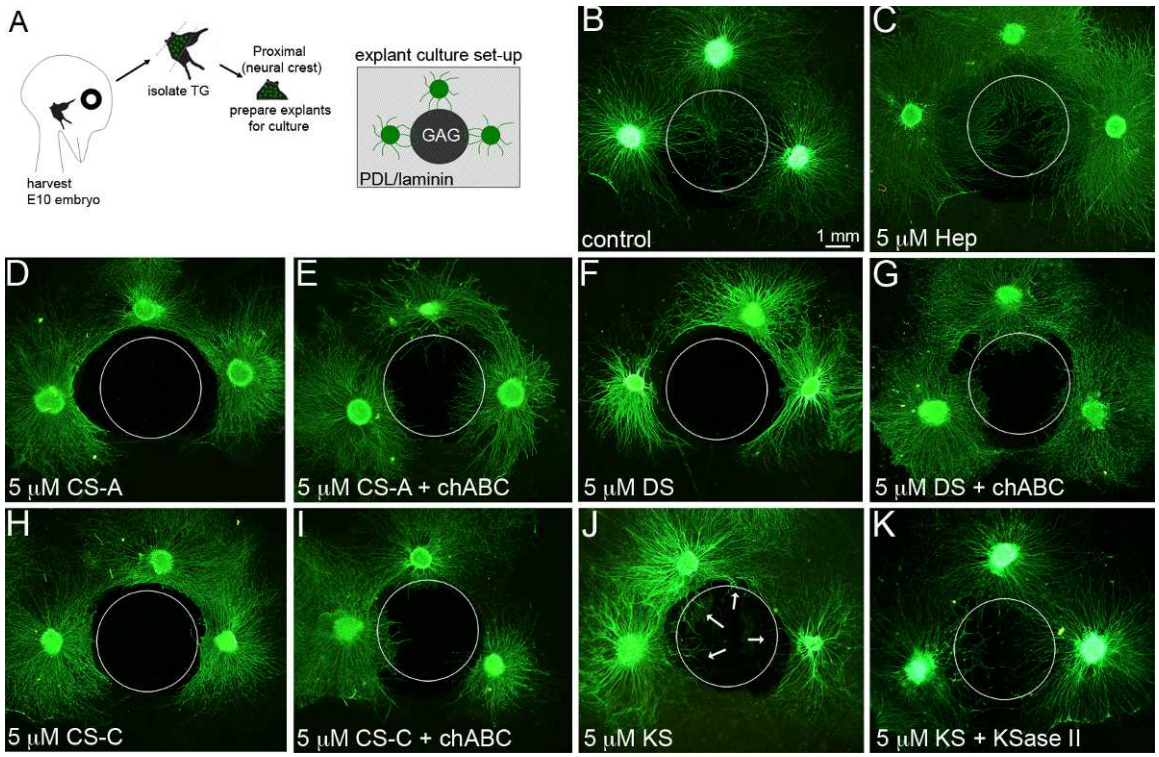


**Figure 5.** Inhibitory potential of immobilized GAG substrates on trigeminal neurite growth. (**A**) Schematic of culture strategy used in this study. Neuronal explants containing primarily neural crest–derived neurons are prepared from the trigeminal ganglia harvested from E10 chick embryos. Trigeminal explants are seeded onto glass slides coated with PDL/laminin and adjacent to an area of the slide where GAG molecules have been spotted. Three explants could be positioned around a single spot. (**B**, **C**) When explants were positioned adjacent to a control spot of water or heparin, neurites from each trigeminal explant grew all around the explant (in a *halo*), including those neurites that grew from the edge of the explant nearest to the spots. Neurites were not impeded from growing over either spot. A *dotted circle* is used in these panels and throughout the figure to show the location of the control or GAG spots in relationship to explant/neurite positions. (**D**–**I**) In contrast, neurites projecting from explants positioned adjacent to a spot of CSA (**D**), DS (**F**), or CSC (**H**) were inhibited from crossing over the spots. The inhibitory effect could be mitigated, first, by treating the spots with chondroitinase ABC enzyme, prior to seeding trigeminal explants (**E**, **G**, **I**). (**J**, **K**) Neurites from explants positioned adjacent to KS spots were partially inhibited (**J**), with a small subpopulation of neurites able to extend onto the spot (*arrows*), whereas the majority of neurites were inhibited; however, treating the spot with KSase II prior to neuronal seeding allowed a higher quantity of neurites to extend over the KS spot. *Scale bar*, 1.0 mm.

the GAG-free side, was recorded for the GAG-substrate side. For instance, percentage values equal to 100% of neurite density on the GAG substrate at the border compared with control substrate indicated equal neurite density between GAG-free and GAG-containing substrate, meaning no inhibition on neurite outgrowth was attributable to the GAG substrate for that condition. Likewise, a percentage value of 50% would indicate that the GAG substrate could impede half (or 50%) of the neurites from extending from the GAG-free substrate and crossing over the boundary and onto the GAG substrate side.

Using these parameters, we first compared neurite outgrowth from trigeminal explants cultured on GAG-free substrate adjacent to a control spot of water, to provide a baseline analysis of how our macro would score neurite outgrowth in the absence of an inhibitory test substrate. In this condition, the water spot yielded a neurite density of approximately 75%, relative to the GAG-free side (Figs. 6A, 6J). Since the explant in our assay is adhered to the GAG-free substrate, any neurites emanating from the explant that would cross over the test substrate (control or GAG) would first need to cross over the GAG-free side. This control percentage value established that in our assay, even if the test substrate is not inhibitory (i.e., water), the neurite density value on the test substrate will be lower than 100% due to the fact that the test substrate side is at a greater distance from the explant than the GAG-free substrate side. Consistent with our qualitative observations that showed that high concentrations of Hep did not impede neurite outgrowth, 5 μM Hep substrates yielded a neurite density of approximately 75% relative to the GAG-free side. Spotting high concentrations of DS and CSC, ranging from 2.5 to 5.0 μM, yielded neurite densities at, or below 1% relative to the GAG-free side, whereas similar concentrations of CSA were not as inhibitory, yielding neurite densities between 3% and 10%. In contrast, KS spots at similar concentrations yielded neurite densities that were low compared with that of controls, but which were significantly higher than that of other GAGs, ranging from 20% to 30%, indicating that DS and CSC were nearly 30-fold more inhibitory to trigeminal neurite growth cone outgrowth than KS. Lowering the concentrations for each GAG further reduced their effect on inhibiting neurite outgrowth in a dose-dependent fashion, indicating that trigeminal neurite growth cones can detect and respond to varying GAG concentrations. Of the four purified GAGs tested in this assay, CSC proved to be the most potent inhibitor to trigeminal neurite outgrowth. This was evident when GAGs were spotted at intermediate levels (0.5–1.0 μM). For instance, when comparing the neurite densities on each GAG substrate spotted at 0.5 μM, CSC yielded a neurite density of approximately 15%, compared with neurite densities of approximately 40% and 50% for similar concentrations of DS and CSA, respectively, whereas the neurite density for 0.5 μM KS exceeded 60%. Finally, low quantities of GAG

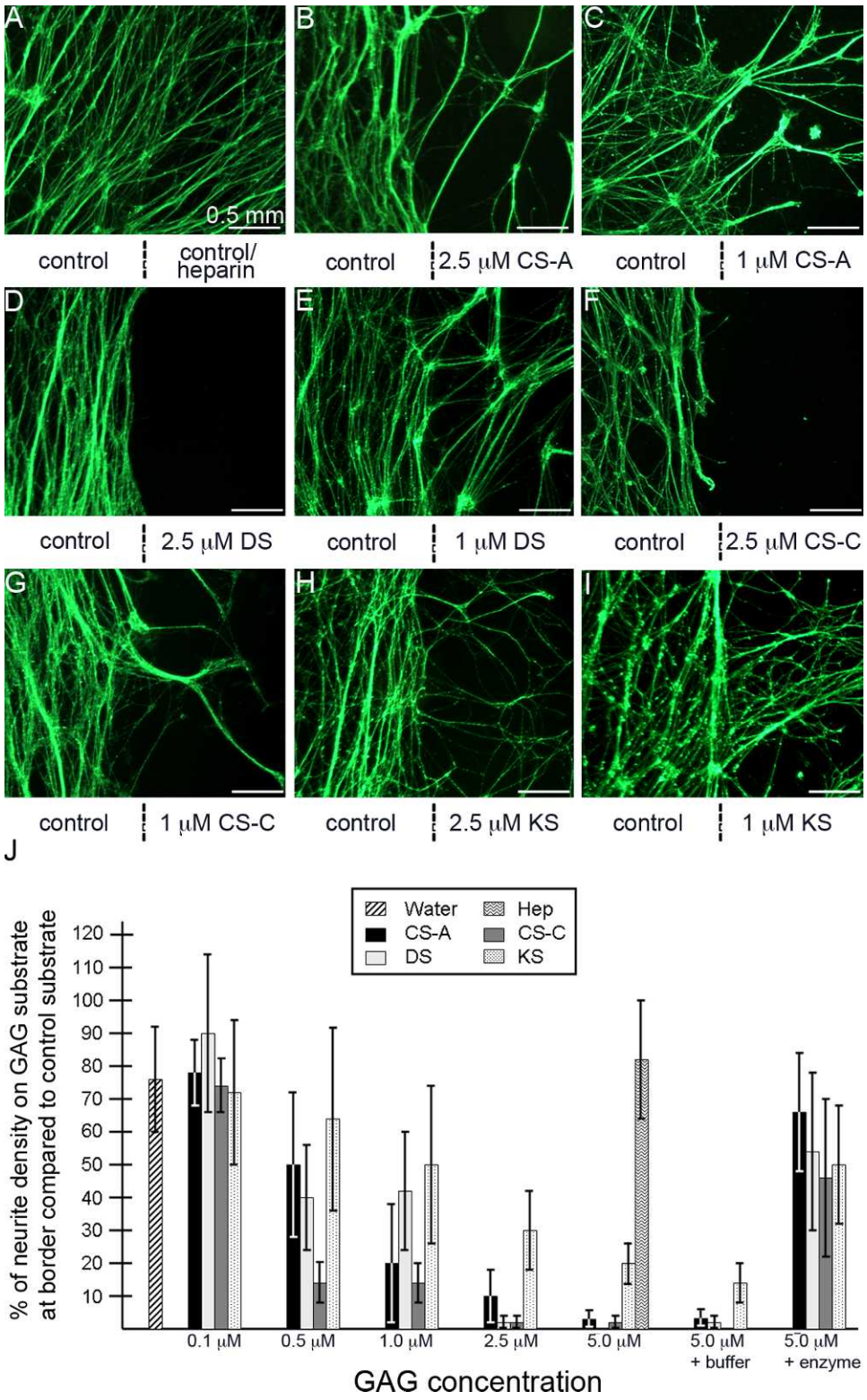


**Figure 6.** Neurite outgrowth in response to varying concentrations of GAG substrates. (**A–I**) High-magnification images show the areas surrounding the spot border. The strategy for generating culture substrates for trigeminal neurons that contain PDL/laminin and GAG or control spots was described in Figure 5A. A *vertical line below the image* indicates the location of the boundary between the PDL/laminin only substrate (control, *left*) and the test substrate (GAG or control spot, *right*). Test substrates and the molar concentration at which they were prepared are also provided *below each image*. Neurites encountering a GAG substrate of CSA (**B**, **C**), DS (**D**, **E**), CSC (**F**, **G**), or KS (**H**, **I**) are inhibited to different degrees, dependent on the type of GAG and concentration (1 μM vs. 2.5 μM), whereas neurites are not inhibited upon encountering a water control or heparin substrate (**A**). (**J**) Percentages of neurite density visible on test substrata for each GAG type and at various concentrations (*right side of the vertical line*) following 3 days of growth as compared with the neurite density visible on the control substrate (*left side of the vertical line*). Refer to the Methods section for further details about how the neurite density values were determined. *Error bars* represent SD. *Scale bar*, 0.5 mm.

**Table 2.** Effects of Individual, Immobilized GAG Molecules on Trigeminal Neurite Outgrowth in an In Vitro Spot Assay

| | Control (No GAG) | 5 μM GAG Only | 5 μM GAG + Buffer | 5 μM GAG + Enzyme | 2.5 μM GAG | 1 μM GAG | 0.5 μM GAG | 0.1 μM GAG |
|---|---|---|---|---|---|---|---|---|
| CS(A) | — | 3.4 ± 3*** | 3.9 ± 2*** | 67.0 ± 19 | 10.9 ± 9***‡ | 18.1 ± 19*** | 51.5 ± 23* | 79.0 ± 13 |
| DS | — | 0.67 ± 0.6*** | 3.0 ± 2*** | 55.4 ± 25 | 1.2 ± 1*** | 43.8 ± 19**‡ | 41.5 ± 16** | 90.5 ± 25 |
| CS(C) | — | 1.3 ± 1*** | 0.7 ± 0.6*** | 45.9 ± 25* | 1.4 ± 1*** | 12.8 ± 6***§ | 12.6 ± 7***§ | 74.4 ± 10 |
| KS | — | 20.0 ± 8***† | 13.5 ± 7***† | 52.1 ± 17* | 29.0 ± 12***† | 50.0 ± 26***‡ | 62.0 ± 30***‡ | 72.8 ± 24 |
| Hep | — | 82.9 ± 20 | — | — | — | — | — | — |
| Water | 73.4 ± 17 | — | — | — | — | — | — | — |

Each numerical value is expressed as mean ± SD and represents the percentage of neurite density visible on test substrata for each GAG at the given concentration when compared with control substrata. These results are also summarized in graphical format in Figure 6J. Pooled data were obtained by analyzing neurite behavior from E10 trigeminal explants cultured adjacent to a minimum of three separate GAG spots per group.

* Significance between neurite density growth on no GAG control (water) and GAG tested is indicated by: significant, * $P < 0.05$; very significant, ** $P < 0.01$; extremely significant, *** $P < 0.001$.

† Indicates a significant increase ($P < 0.05$) in neurite density growth on tested GAG compared with all other GAGs tested (excluding heparin, which was used as control) at identical molarity.

‡ Indicates a significant increase ($P < 0.05$) in neurite density growth on tested GAG compared with some, but not all, GAGs tested at identical molarity.

§ Indicates a significant decline ($P > 0.05$) in neurite density growth on tested GAG compared with all other GAGs tested (excluding heparin, which was used as control) at identical molarity.

spots (0.1 μM) allowed neurites to freely cross over each GAG substrate at levels similar to those reported for water controls. Overall, the percentages for neurite density for each substrate condition and relevant statistical analyses are summarized in Figure 6J and also provided in Table 2.

The data from the in vitro spot analyses discussed above clearly indicate that individual types of GAGs are differentially inhibitory to trigeminal neurite growth cone outgrowth. However, since these analyses were performed using a static approach where qualitative and quantitative observations were gathered at a representative endpoint of neurite outgrowth behavior 3 days after seeding explants onto the prepared substrates, we had not specifically addressed how GAGs influenced trigeminal neurite behavior. For this reason, we next chose to examine growth cone morphology and behavior of the neurite tip/growth cone, in a time-lapse microscopy study, as it contacted high concentrations of CS/KS (data not shown) and DS (shown in Fig. 7). We collected images of growth cone morphology, every 12 hours, beginning just prior to the time when the growth cones were to contact the DS-rich substrate region. Growth cones contacting DS often stopped or stalled upon contact with the GAG, with the growth cone remaining on the GAG-free side of the border instead of migrating over the immobilized-GAG substrate, or retracting (Fig. 7E). Prior to growth cones contacting DS, neurites from the same explants advanced directly toward the spot without pausing, indicating that the stop/stall growth cone phenotype was due to the presence of DS. Once stalled on the GAG-free substrate, near the DS spot, growth cones appeared spread out and extended filopodia outward to sample the varying substratum (Fig. 7E′; arrows). In contrast, growth cones extending on GAG-free surface or on a control water spot advanced without pausing and never displayed growth cone stalling and spreading (Figs. 7A–C). Stalled growth cones eventually began to turn at the border of the DS spot and extend their neurites along the edge of the border, invariably on the GAG-free side (Figs. 7E″, 7F″, arrowheads). Neurites advancing along the GAG substrate border grew without pausing and displayed growth cones that were reminiscent of those extending on GAG-free surface toward the spot (arrowheads, Figs. 7D″, 7E″, 7F″). Like DS, growth cones showed similar morphology when encountering GAG spots derived of CS and KS at high concentrations (data not shown). These time-lapse images indicated that the migratory path of trigeminal neurite growth cones could be redirected by GAGs, inducing them to stall while filopodia from those growth cones determined a more preferred substrate, to which they then would turn and proceed to advance upon. These data, when combined with prior data revealing the presence of GAGs in the developing eyefield, suggest that GAGs deposited in defined regions of the eye may alter and direct nerve pathfinding.

## CS, DS, and KS Presented in Soluble Form Did Not Influence Trigeminal Neurite Outgrowth

Reported differences between the effects on neurite outgrowth by immobilized and soluble PGs and GAGs led us to examine the inhibitory potential of each GAG in soluble form, to allow direct comparison with responses to the immobilized forms above.[8,13,38] Such differences may be attributed to a difference in PG or GAG conformation, in turn altering their ability to interact with neurite growth cone receptors and may shed insight into the mechanism by which GAGs regulate neurite growth cone behavior in vivo, since growth cones may encounter PGs or GAGs in varying forms in vivo, such as bound to a cell surface or to ECM (immobilized) or as soluble molecules diffusing through the ECM.

To assess the role of soluble GAGs on trigeminal neurons, the neurite outgrowth pattern was analyzed by determining the average length of the 8 to 10 longest neurites per trigeminal explant when GAGs were presented in soluble form to cultured trigeminal explants. In contrast to our earlier findings using immobilized GAG substrata, we found that the presence of soluble GAGs did not change the morphology or the diameter of the neuritic halo following 2 days of culture on PDL/laminin substrate, even at high concentrations (Fig. 8A). These findings are in accord with those of Snow et al.,[38] who reported that soluble CSPGs caused no detrimental effect on outgrowth of embryonic sensory neurons (derived from dorsal root ganglia [DRG]) when neurons were grown on laminin substrate. The same report also found that the DRG growth cones could be affected by soluble CSPGs if the neurons grew on a fibronectin substrate, indicating that neurons may behave differently in the presence of soluble GAGs or proteoglycans when grown on different substrata.[38] For this reason, we grew trigeminal explants within a three-dimensional matrix composed of soluble GAGs and collagen I. Collagens are the most abundant proteins in the corneal stroma and surrounding mesenchymal ECM, with collagen I

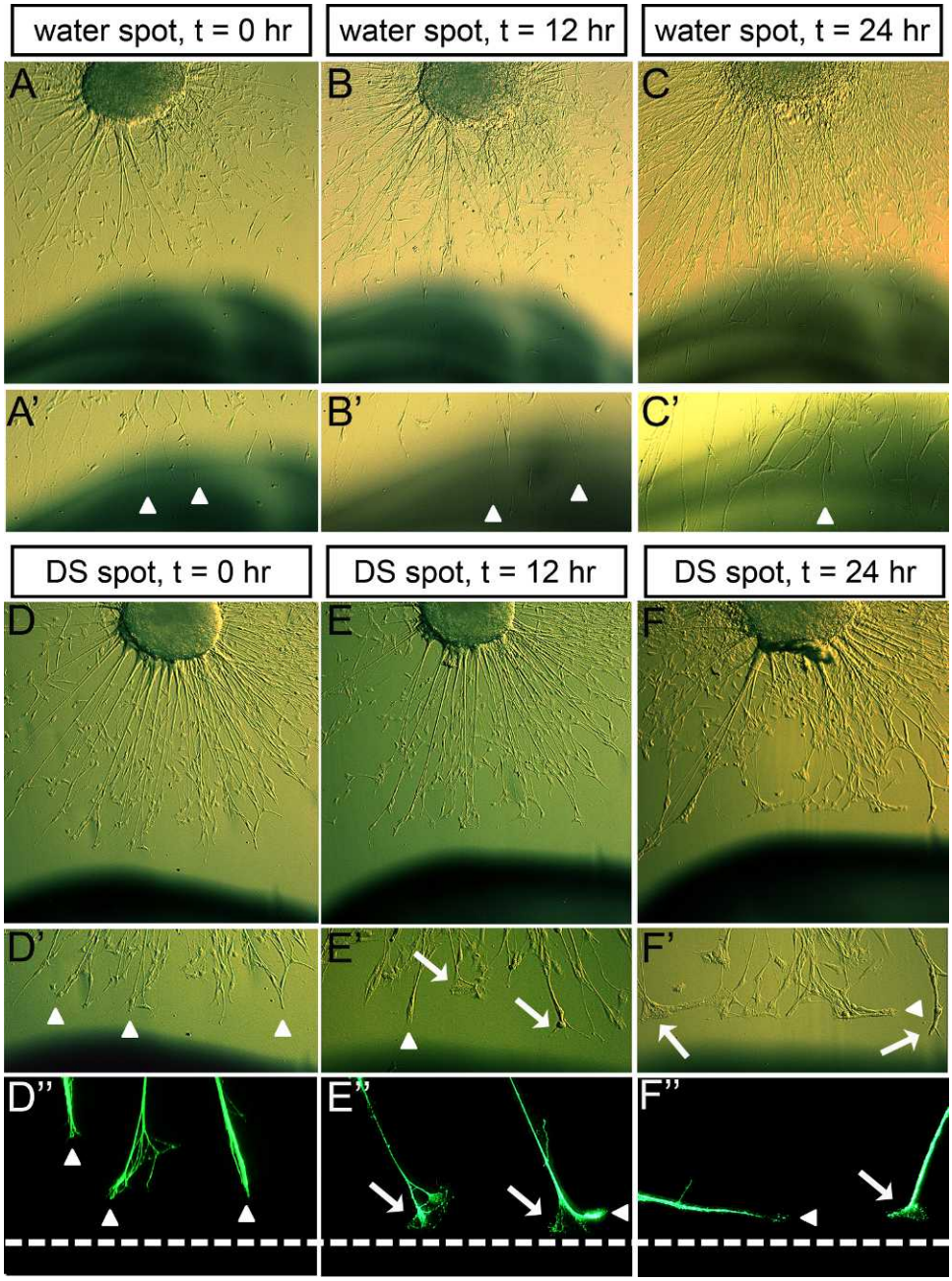


**Figure 7.** Growth cone morphology upon contact with immobilized GAG substrate. (**A–F**) Time-lapse images of trigeminal growth cones contacting a water spot (control) (**A–C**) or an area rich in DS (**D–F**), while extending on a GAG-free, neuronal-supportive (PDL/laminin) substrate, on either 0 (**A**, **D**), 12 (**B**, **E**), or 24 (**C**, **F**) hours after the start of imaging. (**A–C**) Brightfield, phase-contrast images of live explants and their neurite projections toward a water spot show that neurites advance over the spot unimpeded and growth cones migrate without pausing, or spreading (*arrowhead* denotes advancing, unspread growth cone). (**D–F**) Brightfield, phase images of live explants and their neurite projections (**D–F**, **D′–F′**) or fluorescent images of fixed explants and their neurite projections (**D″–F″**), toward a DS spot show that neurites advance unimpeded and growth cones are not spread out prior to contacting the DS spot (**D′**, **D″**, *arrowheads*), but that upon contacting DS-rich substrate, growth cones stop/stall and become spread out with extended filopodia (*arrow* denotes spreading growth cones), before turning and advancing along the DS border (*arrowheads* in **E″**, **F′**, **F″**). *Dotted lines* (D″–F″) represent the border between GAG-free substrate and GAG/control substrate.

being the predominant type, making this substrate a more in vivo–like setting for examining trigeminal outgrowth in our studies. Similar to growth on laminin, no differences in neuritic outgrowth following 2 days in culture within collagen matrices were observed between explants grown in the presence of GAGs or in control (GAG-free) conditions (Fig. 8B). These findings indicate that the inhibitory nature of purified, immobilized GAGs on the migration of trigeminal neurite growth cones is not detected when GAGs are presented to neurons in a soluble form.

## Effect of CSA/C, DS, and KS on Trigeminal Neurite Fasciculation and Branching

In the present study we showed that varying the concentrations of immobilized GAGs resulted in different degrees of

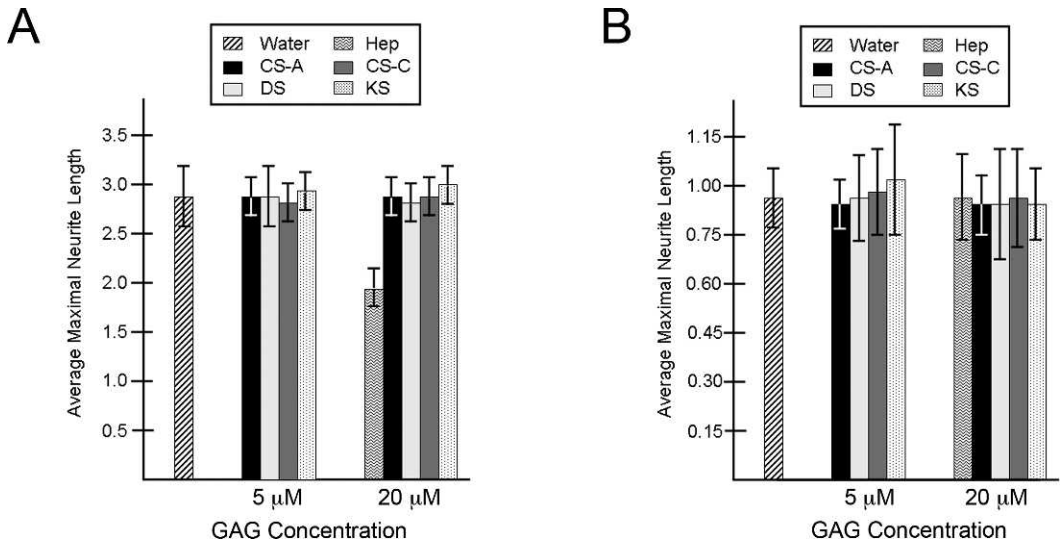


**Figure 8.** Trigeminal neurite outgrowth in the presence of soluble GAGs. (**A**, **B**) Neurite outgrowth in the presence of soluble GAGs from trigeminal explants grown on PDL/laminin (**A**) or in a collagen I matrix gel (**B**) for 2 days. For a single explant within each culture condition, 8 to 10 of the longest neurites were identified and measured to derive a mean length (in mm) of the longest neurites for that explant. Histogram values are expressed as the mean neurite length (in mm) among a group of explants that were scored independently ($n = 6$–10 explants per condition). *Error bars* represent SD.

neurite elongation on the surface of the GAG-bound substrate (see Fig. 5). Notably, intermediate concentrations (0.5–1.0 μM) of a given GAG spotted on PDL/laminin provided a favorable substrate on which a subset of neurite growth cones from the adjacent trigeminal explant could elongate onto the GAG spot, whereas the growth cones of other neurites were deflected at the GAG spot border. Using this culture paradigm, we observed the behaviors of individual trigeminal neurite growth cones as they extended on the surface of different purified GAGs and found differential effects on fasciculation and branching of neurites, dependent on the type and concentration of immobilized GAG substrate. Neurite fasciculation behaviors were quantified by determining the percentage of thin (0.4–1.2 μm; nonfasciculated), intermediate (1.3–4.0 μm), and thick (4.1 μm or thicker; fasciculated) neurites that elongated onto the immobilized GAG surface.[86,87] Additionally, the number of defasciculation/branch points for each neurite that had extended on the GAG surface was recorded. When trigeminal explants were grown on controls, a water spot dried on PDL/laminin, neurites primarily grew as intermediate fascicles with 1 to 2 points of branching or defasciculation per neurite (Fig. 9A). A predominance of intermediate to thick fascicles was apparent among neurites extending on surfaces coated with CSA/C or DS (Figs. 9B–D). Moreover, the majority of fascicles elongating on either of these two substrata grew without branching or defasciculating (Figs. 9B–D). In contrast, growth on a KS substrate was markedly different from all other conditions, in that neurites were nonfasciculated and highly branched (Fig. 9E). The effects of each purified GAG on neurite fasciculation and branching are summarized in Figures 9F and 9G. The effects of purified, immobilized GAGs on neurite behavior and morphology reported here were consistent among different GAG concentrations tested, with maximal effects on fasciculation/branching when intermediate concentrations were used, wherein approximately 15% to 50% of neurites emanating from explants could cross over the GAG substrate. Decreasing the concentration of GAGs by a factor of one-fifth to one-half allowed significantly higher quantities of neurites to elongate onto the GAG substrate, making individual observations of individual neurite behaviors grown under these conditions difficult. Collectively, these qualitative and quantitative observations reveal that trigeminal neurite fasciculation and branching behaviors are influenced differentially by specific types of GAG molecules and in a concentration-dependent manner, suggesting that such nerve bundling behavior could be expressed by nerves in vivo as they enter the eyefield and first encounter limbal and then corneal stromal GAGs, in both cases in their normal immobilized forms.

## Discussion

During chick embryonic development, beginning at E4, nerves extend from the OpV branch of the TG toward the developing cornea.[72] Upon arriving at the edge of the corneal stroma, nerves are delayed from entering it for several days due to the presence of inhibitory Semaphorin and Slit molecules in the cornea.[69,72] Instead, nerve fibers split into a dorsal and a ventral stream, eventually forming a complete pericorneal nerve ring in the limbus mesenchyme that surrounds the periphery of the corneal stroma.[60] Data collected in the current study show that, beginning at E9, nerves exit the nerve ring as tight fascicle bundles, and that their growth cones advance through the limbus mesenchyme in that bundled form as they migrate toward the corneal stroma without bifurcating or branching. Nerves penetrate the anterior stroma at E9 to E10 and immediately begin to bifurcate/branch repeatedly as their growth cones migrate through the stroma toward the epithelium, which they penetrate by E12. A recent report showed that once nerves arrive at the epithelium, they branch repeatedly and form synapses with epithelial cells.[89]

Nerve growth cone guidance during development and regeneration arises from a balance of inhibitory and promotional cues in the local environment consisting of several ECM molecules, cell adhesion molecules, neurorepellant molecules, chemoattractants, and growth factors, some soluble and diffusible but many immobilized in the ECM.[90–94] To date, studies of the mechanisms underlying nerve growth and patterning during both avian and mouse cornea innervation have been limited to those concerned with axon growth cone inhibition as a result of the high degree of neurorepellant molecules in the eyefield secreted by the lens and cor-

nea.[69,72,95] Extracellular GAG molecules are known to influence sensory nerve growth and guidance during embryonic development,[55,56,96] prompting us to examine the potential roles for ECM–GAGs in cornea innervation in this study. A prior study by our group showed that CS, DS, and KS are the predominant ECM–GAGs produced in the cornea during corneal innervation stages.[64] Conversely, expression of heparan sulfate (HS), another ECM–GAG, is high in the cornea during early development but dramatically reduces in the cornea many days prior to cornea innervation and remains low throughout cornea development,[64] making HS a minimal component of the cornea ECM during innervation. ECM–GAG expression data collected from this study led our group to speculate on the potential roles for CS, DS, and KS on cornea innervation.

Examining the distributions of CS, DS, and KS GAGs by immunolabeling during cornea innervation revealed that these sulfated epitopes are developmentally regulated throughout chick cornea development. Strikingly, at each developmental day examined, CS-56 (CSA/C) and 7D4 (CS/DS) immunoreactivities were localized among cells in the limbus and corneal tissues that were avoided by growing TG nerve growth cones during innervation. CSA and CSC were primarily localized to the anterior layers of the limbus at E9, but were absent from the posterior limbus and all corneal layers at this stage. By E10, CS-56 (CSA/C)–positive epitopes appeared in the medial layers of the corneal stroma, with positive staining appearing gradually in more posterior stromal layers during subsequent days of development (E11–E14). Staining patterns of 7D4 (CS/DS) during E9 to E14 were similar to those of CS-56 (CSA/C), with the exception of the appearance of 7D4-positive epitopes in the medial layers of the corneal stroma at E9, a day earlier than CS-56 immunolabeling. Because 7D4 detects DS epitopes in addition to CSA/C epitopes, we reason that 7D4 immunoreactivity in E9 corneas represents the presence of DS chains in E9 corneas.

Immunodetection of highly sulfated KS epitopes in this study was carried out using I22 and 5D4 antibodies. Results obtained with I22 were similar to those obtained with 5D4 at each embryonic day examined. KS epitopes were present throughout the corneal stroma from E9 to E14, but were absent from corneal epithelium and limbus mesenchyme. We report here that KS antibody staining was uniform throughout all stromal layers of the chick cornea by E10 to E11, whereas a previous report by our group concluded that KS staining did not appear in the more anterior layers prior to E12 to E16.[63] Increased corneal KS staining in the current study may be explained by usage of confocal microscopy to detect sulfated epitopes, which is likely more sensitive than epifluorescence techniques used in the prior study. More recently, Young et al.[66] reported that 5D4 was preferentially expressed in anterior stroma at E10 to E14. Differences between their findings with those of Funderburgh et al.[63] and ours may be due to tissue processing prior to antibody staining. In this study and that of Funderburgh et al.,[63] corneas were fixed and embedded in paraffin, prior to washes in detergent-containing saline and antibody stainings, whereas in Young et al.,[66] cornea specimens were unfixed and frozen, then subjected to detergent-containing saline washes prior to staining.

The cornea contains the proteoglycan decorin containing chondroitin/dermatan sulfate (CS/DSPG) and three proteoglycans containing keratan sulfate (KSPG), which are lumican, keratocan, and mimecan.[2] Each of these proteoglycan core proteins may contain the CS/DS or KS molecules whose expression we analyzed in the developing eyefield in this study. Decorin expression overlaps that of CS/DS in the cornea matrix during stages of stromal invasion to the cornea,[97] time points that preceded those examined in this study. It is likely that decorin expression also overlaps with CS/DS expression in the cornea and pericorneal tissues during cornea innervation; however, to our knowledge its expression has not been examined in the chick cornea during such stages. The KSPGs lumican, keratocan, and mimecan are detectable by RT-PCR at high levels during cornea innervation stages in the chick, relative to their expression in the adult, and each of those three core proteins is modified with KS GAG chains in the embryonic cornea.[98] Lumican is the most abundant KSPG during cornea innervation, whereas mimecan is the least abundant KSPG during cornea development.[98] We have previously reported in situ hybridization data for the two major core proteins keratocan and lumican in the cornea.[99] Both core proteins are expressed in the cornea stroma and endothelium, but absent from the epithelium at E8 to E9. Lumican expression is more widespread in the corneal edges and limbus, whereas keratocan expression is exclusive to corneal regions.[99] These core protein expression patterns are complementary in the developing cornea to KS (as shown in this study) and so it is likely to presume that these are important GAG-bearing cores in the cornea at these stages.

It is well established that CS- and KSPGs in the ECM have crucial roles in modulating axonal growth and guidance during development and also after nervous system injury. Although much evidence has accumulated suggesting that it is the GAG chain moieties that are recognized by nerve growth cones, fewer studies have specifically addressed the differential effects that individual GAG moities have on a particular nerve cell.[13,20,22,46,47,100,101] Here, we used a modified spot assay designed to mimic an in vivo environment whereby GAGs are immobilized and presented solely to nerve growth cones, but not to their neuronal cell bodies, similar to how GAGs would be encountered by growth cones in a developing embryo. Our results show that each GAG tested in the study displayed its own unique potential for inhibiting trigeminal nerve growth cone migration in vitro. CS, DS, and KS GAGs induced trigeminal growth cones to stop on the GAG-free surface, near the GAG border, and oftentimes growth cones would turn at the border to avoid crossing over the GAG surface. Growth cone turning to avoid inhibitory substrates is mediated by reversible changes in actin filament bundles and microtubule dynamics in the growth cone tip.[102,103] It has been previously shown that DRG growth cones contacting immobilized, neural-derived CSPG interfaces stall and turn without growth cone collapse, which is characterized by a breakdown of F-actin at the growth cone tip.[104] Rather, actin-based filopodia at the growth cone continuously extend around the growth cone to sample the surrounding substrata. Eventually after a sampling period, the growth cone turns in the direction of filopodia extended on a favorable substrate to avoid the inhibitory CSPG,[104] indicating that CSPG induces dynamic changes to F-actin and cortical actin at the growth cone, rather than actin disassembly, resulting in growth cone steering. We observed here that growth cones of trigeminal neurons did not collapse upon contact with GAGs and display similar turning behavior to DRGs in response to inhibitory GAGs, suggesting that actin dynamics are similar between TG and DRG neurons. In addition, it was recently reported that PC-12 neurons contacting a CSPG interface display a decrease in the rate of microtubule polymerization.[105] Interestingly, the change in microtubule dynamics occurs exclusively at the neurite growth cone tip in direct contact with the CSPG substrate, whereas neurites of the same cell body that do not contact CSPG display normal microtubule dynamics.[105] These studies indicate that proteoglycans/GAGs influence the cytoskeleton dynamics of neurites in a dynamic and localized fashion, accounting for the stalling and steering growth cones at inhibitory interfaces. In the future, to better characterize the inhibitory mechanisms of

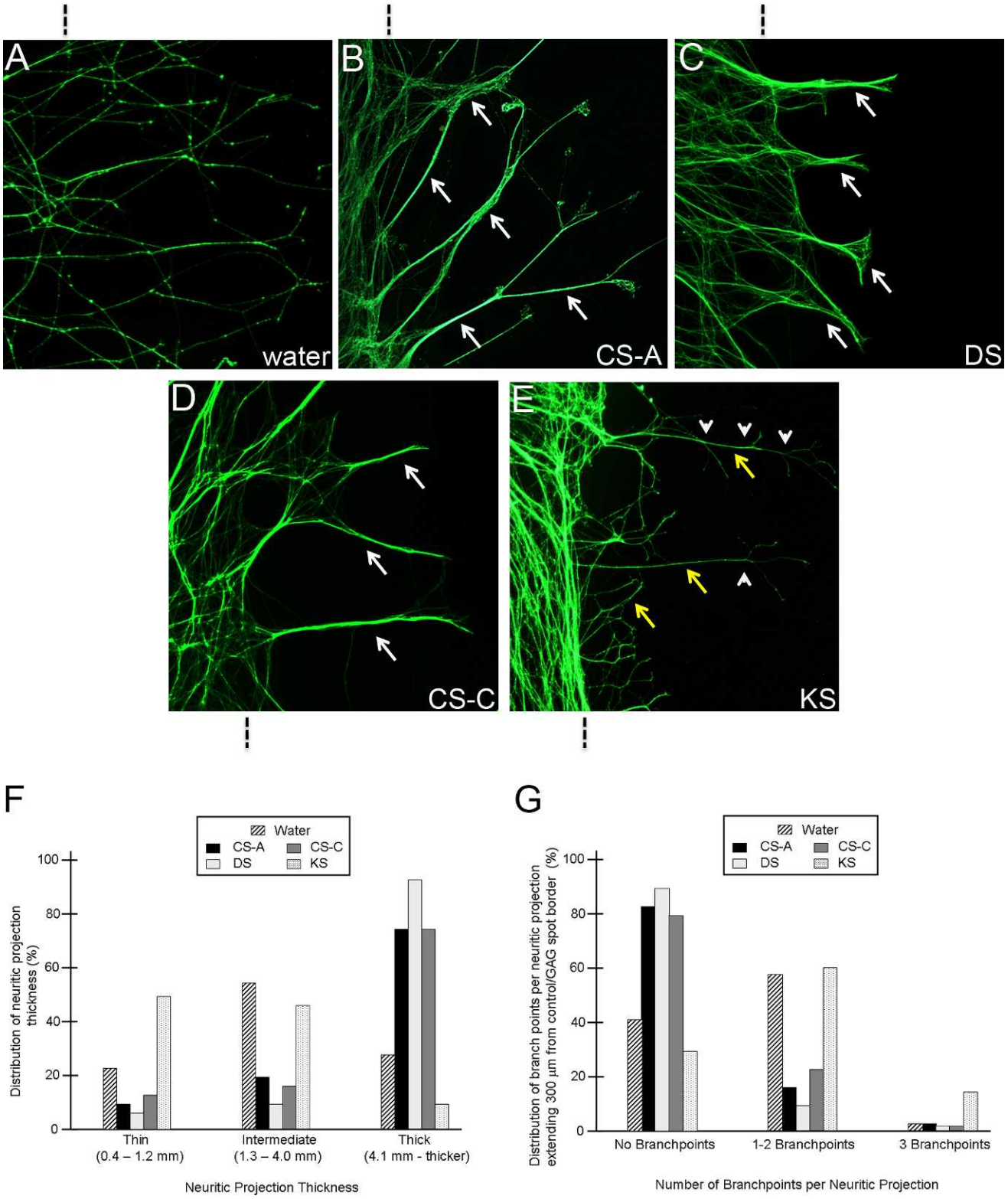


**Figure 9.** Trigeminal neurite behavior following elongation upon intermediate, permissive concentrations of immobilized GAG substrates. (**A–E**) The strategy for generating culture substrates so that trigeminal neurons grow out on surfaces containing PDL/laminin and GAG or control spots was described in Figure 5A. A *vertical line above* (**A–C**) or *below* (**D**, **E**) *the image* indicates the location of the boundary between the PDL/laminin only substrate (control, *left*) and the test substrate (GAG or control spot, *right*). Representative images are shown for neurites encountering a water control spot (**A**) or CSA (**B**), DS (**C**), CSC (**D**), or KS (**E**). Neurite behavior upon growing over CSA (**B**), DS (**C**), and CSC (**D**) is characterized by a marked shift from intermediate to thick fascicles (*white arrows*, fasciculation) and reduced defasciculation/branching. On the contrary, neurite behavior seen when growth cones migrate upon KS (**E**) is characterized as nonfasciculated (*yellow arrows*, nonfasciculated) with a high degree of branching (*white arrowheads* represent points of branching or defasciculation). (**F**) Percentages of neurites that grew as fasciculated or nonfasciculated under control and test conditions. (**G**) Percentages of branching points per neurite under control and test conditions. *n* values: water, 89 neurites; CSA, 127 neurites; DS, 114 neurites; CSC, 110 neurites; KS, 174 neurites.

individual GAG moieties on trigeminal outgrowth, it will be important to study cytoskeletal dynamics in trigeminal growth cones as they contact individual GAG moieties in vitro.

Among the four GAGs tested in this study (CSA/C, DS, and KS), trigeminal growth cone outgrowth seemed to be inhibited most by CSC. Between the two other GAGs, DS was more inhibitory than CSA to growth cone movement at high concentrations, but less inhibitory at lower concentrations. Interestingly, we found that KS was much less inhibitory to movement of trigeminal growth cones than were CS and DS molecules. Partial inhibition of trigeminal neurites by KS was evident only at the highest concentrations tested (i.e., 2.5 and 5 μM). Even at these concentrations, considerable neurite growth was evident on KS substrates, whereas similar concentrations of CSC and DS GAGs induced complete inhibition of trigeminal neurite outgrowth, suggesting that KS may be a weak inhibitor of trigeminal neurite outgrowth, whereas CS and DS are strong inhibitors. Collectively, these findings highlight the specificity with which trigeminal nerve growth cones can detect and respond to differences in component disaccharide structure, sulfation, and concentration between different GAGs.

Our in vitro studies strongly support the hypothesis that CS and DS molecules in the embryonic limbus and corneal stroma may, themselves, serve as a barrier to growth cone advancement during chick cornea innervation, irrespective of the presence of other neuroinhibitory molecules diffusing through, or bound to, the ECM[94] (none was purposely added during in vitro experiments here). The presence of CS/DS in the medial and posterior cornea stroma layers during stages of cornea innervation could help to explain why these stromal tissues remain free of trigeminal nerves, whereas more anterior stromal layers that lack CS/DS become populated by nerves. Furthermore, the late appearance of CS/DS in the limbus during eye development seems to be consistent with the possibility that these GAGs act to inhibit further immigration of neuronal growth cones into the corneal stroma once a certain number of nerves have crossed the anterior corneal basement membrane and formed synapses with epithelial cells.[89] On the other hand, our finding here that nerves advanced into regions of the cornea where KS was localized indicates that corneal KS is not sufficient to impede the advancement of incoming trigeminal nerves. This further supports the finding that KS is a weaker inhibitor of trigeminal nerve growth cone migration, compared with CS/DS. Because high KS concentrations are required to inhibit trigeminal neurites in vitro (this study), it is possible that KS is not present at high enough levels in the embryonic cornea to impede nerve advancement.

In the present study we also examined whether GAGs could inhibit trigeminal neurite outgrowth when they were presented in soluble form. In contrast with using immobilized GAGs, data collected here indicated no difference in neurite outgrowth from trigeminal explants when they were challenged with CS, DS, or GAGs that were presented to them in the culture media. This may suggest that trigeminal growth cones can sense how GAGs are presented, potentially by detecting conformational differences between immobilized versus soluble form, and inducing a behavioral effect. Alternatively, the radical difference in growth cone behavior in response to surface-bound GAG versus soluble GAG may arise from a difference in the effective, final concentration of that same GAG that is exposed to the growth cone. This would assume that GAGs bound to the culture surface are more concentrated than when they are free-floating in solution. We attempted to address this potential explanation in our studies by culturing trigeminal explants with soluble GAGs at concentrations 10× higher than those effective at influencing trigeminal outgrowth when GAGs were bound to the surface (i.e., 2 μM for immobilized study versus 20 μM for soluble study). Despite this we never detected an effect of soluble GAGs on trigeminal outgrowth, regardless of concentration tested, making it difficult to conclude which of the above potential hypotheses could help to explain the difference between immobilized GAG versus soluble GAG on trigeminal outgrowth in our study. One final possibility that may account for the differences in trigeminal growth when challenged with GAGs in immobilized versus soluble form may be due to differences in how the neuronal cells encounter the GAGs in our study. When trigeminal explants are grown adjacent to immobilized GAG spots, only the growth cones are exposed to the GAG, but the cell bodies are not. Moreover, growth cones are given a choice of whether to advance over GAG surface or stop/turn and grow on GAG-free substrate. In contrast, when GAGs are presented in soluble form, the neurites and cell bodies, in addition to the growth cone, are exposed to the GAGs. Snow et al.[8] showed that neurites from DRG explants were strongly repelled from immobilized CSPGs if the explants were cultured on GAG-free substrata and the nerve growth cones encountered the CSPGs, but not if the neuronal cell bodies were exposed to CSPGs, even when immobilized. This indicates that neurite behavior can be greatly influenced not just by the ECM encountered by the growth cone, but also by the ECM surrounding the cell body.

Fasciculation and branching depend on adhesive and repulsive interactions between growing axons and the surrounding nonneuronal cells and ECM environment encountered by the axons. These collective influences help to determine the growth-cone decisions to follow a "pioneer axon," or an existing fascicle, or to diverge from it. In the chick embryo, removal of repulsive polysialic acid (PSA) moieties on neural cell adhesion molecules (NCAMs) leads to increased axon bundling/fasciculation and a marked reduction in branching of peripheral nerves.[106–109] The presence of PSA-NCAM in developing chick corneas suggests a similar role in nerve growth during cornea innervations.[110] Additionally, axon–axon adhesion may also contribute to fasciculation and branching regulation. In this vein, altering Nogo-A signaling in vitro and in vivo upon inhibiting Nogo-A signaling negatively affects axon–axon adhesion and increases fasciculation.[86] Despite recent reports indicating the importance of GAGs to axonal fasciculation and branching, direct requirements for ECM–GAG moieties in regulating these nerve behaviors are poorly understood. DRG sensory neurons grown on laminin and an intermediate, permissive concentration of CSPGs displayed neurite outgrowth that was predominantly fasciculated.[6] Data presented in the current report extend the studies by Snow and colleagues[6] using CSPGs as we have examined the effect on sensory neuron fasciculation of purified CS and DS GAG moieties, lacking the proteoglycan core protein. We show here that CSA, CSC, and DS can each individually trigger neurite fasciculation. In sharp contrast, neurites growing on KS were highly branched and grew predominantly in nonfasciculated arrays. In contrast to our studies using sensory neurons of the PNS, rat CNS embryonic cortical neurons did not display increased fasciculation when growth cones were presented with the same purified, commercial preparation of CSA as was used in our study.[13] Moreover, immobilized, purified CSA and KS were shown to significantly increase CNS dopaminergic (DA) neurite branching on poly-L-ornithine.[46] Collectively, data from these studies and ours indicate that the differential effects on neurite behavior when encountering immobilized GAGs, likely depends on the source of the neuron (PNS versus CNS), as well as on the actual charge density/GAG density on the surface. A further factor that may influence neurite responses to GAGs during in vitro assays is the choice of growth substrate surrounding the GAG. In support of this, Macé et al.[46] reported

that the branching effect of CSA, but not that of KS, on DA neurons grown on poly-L-ornithine was significantly reduced when neurons were grown instead on laminin, thus making their experimental protocol and data similar to those in the current study, in both of which GAGs were presented to growth cones in combination with laminin. Many lines of evidence in addition to this investigation support the notion that CS- and KS-GAGs are colocalized with laminin in vivo in the developing cornea[97,111] and other tissues,[112,113] supporting the biological relevance of the substrate molecules chosen in this study.

The in vitro evidence that CS and DS support trigeminal sensory neuron fasciculation is consistent with nerve growth behavior in vivo during eye development. The cornea and limbus express CSPGs, as do other components of the optic pathway, including the retina.[9,25] The expression of CSPGs in these tissues is developmentally regulated and CSPG expression is inversely related to the position of ingrowing axons during innervation of the chick cornea (this study) and in the rat and chicken retina.[9,25] We found that nerve growth was predominantly fasciculated in the limbus, a tissue rich in CS and DS molecules, and poor in KS, consistent with highly fasciculated nerve growth in the chicken retina, which is also rich in CSPGs.[9] In sharp contrast, nerve processes in the anterior stroma, which is rich in KS, were nonfasciculated and highly branched. Consistent with this, developing retinal processes in the rat retina (i.e., CNS nerves), expressing low levels of CSPGs, are mostly nonfasciculated.[25] These in vivo growth behaviors in the developing eye directly correlate with the in vitro data presented in this investigation.

Corneal nerves provide important protective and trophic functions. Disruptions to corneal nerves, as a result of trauma or corrective surgery, may lead to altered epithelial morphology and function, delayed wound healing, and reductions in tear film formation.[114–117] Despite this, little is known concerning the mechanisms of cornea innervation or how to activate regeneration of the cut ends of corneal nerves once they become damaged. Results from this study suggest that the GAG molecules prevalent in the ECM of developing eyes play a role in the guidance of nerves during cornea innervation. Consequently, the ECM of the cornea should be considered when determining mechanisms to transiently stimulate nerve growth in posttransplantation cornea treatments and post-LASIK nerve regeneration.

## Acknowledgments

The authors thank Abigail H. Conrad for insightful discussion at the onset of this work, and Peter Y. Lwigale and members of Gary W. Conrad's laboratory for support and advice during the duration of this work. Imaging services were provided by the Research Resources Center–Research Histology Core at the University of Illinois at Chicago established with the support of the Vice Chancellor of Research.

## References

1. Tosney KW. Cells and cell-interactions that guide motor axons in the developing chick embryo. *Bioessays*. 1991;13:17–23.
2. Gipson IK, Joyce NC, Zieske JD. The anatomy and cell biology of the human cornea, limbus, conjunctiva, and adnexa. In: Foster CS, Dohlman CH, eds. *Smolin and Thoft's The Cornea: Scientific Foundations and Clinical Practice*. 4th ed. Philadelphia: Lippincott Williams & Wilkins; 2005:3–37.
3. Davidson EA, Meyer K, Chondroitin, a new mucopolysaccharide. *J Biol Chem*. 1954;211:605–611.
4. Meyer K, Linker A, Davidson EA, Weissmann B. The mucopolysaccharides of bovine cornea. *J Biol Chem*. 1953;205:611–616.
5. Margolis RU, Margolis RK. Chondroitin sulfate proteoglycans as mediators of axon growth and pathfinding. *Cell Tissue Res*. 1997;290:343–348.
6. Snow DM, Smith JD, Cunningham AT, McFarlin J, Goshorn EC. Neurite elongation on chondroitin sulfate proteoglycans is characterized by axonal fasciculation. *Exp Neurol*. 2003;182:310–321.
7. Bandtlow CE, Zimmermann DR. Proteoglycans in the developing brain: new conceptual insights for old proteins. *Physiol Rev*. 2000;80:1267–1290.
8. Snow DM, Lemmon V, Carrino DA, Caplan AI, Silver J. Sulfated proteoglycans in astroglial barriers inhibit neurite outgrowth *in vitro*. *Exp Neurol*. 1990;109:111–130.
9. Snow DM, Watanabe M, Letourneau PC, Silver J. A chondroitin sulfate proteoglycan may influence the direction of retinal ganglion cell outgrowth. *Development*. 1991;113:1473–1485.
10. McKeon RJ, Schreiber RC, Rudge JS, Silver J. Reduction of neurite outgrowth in a model of glial scarring following CNS injury is correlated with the expression of inhibitory molecules on reactive astrocytes. *J Neurosci*. 1991;11:3398–3411.
11. Dou CL, Levine JM. Inhibition of neurite growth by the NG2 chondroitin sulfate proteoglycan. *J Neurosci*. 1994;14:7616–7628.
12. Friedlander DR, Milev P, Karthikeyan L, Margolis RK, Margolis RU, Grumet M. The neuronal chondroitin sulfate proteoglycan neurocan binds to the neural cell adhesion molecules Ng-CAM/L1/NILE and N-CAM, and inhibits neuronal adhesion and neurite outgrowth. *J Cell Biol*. 1994;125:669–680.
13. Karumbaiah L, Anand S, Thazhath R, Zhong Y, McKeon RJ, Bellamkonda RV. Targeted downregulation of N-acetylgalactosamine 4-sulfate 6-O-sulfotransferase significantly mitigates chondroitin sulfate proteoglycan-mediated inhibition. *Glia*. 2011;59:981–996.
14. Smith-Thomas LC, Fok-Seang J, Stevens J, et al. An inhibitor of neurite outgrowth produced by astrocytes. *J Cell Sci*. 1994;107:1687–1695.
15. Smith-Thomas LC, Stevens J, Fok-Seang J, Faissner A, Rogers JH, Fawcett JW. Increased axon regeneration in astrocytes grown in the presence of proteoglycan synthesis inhibitors. *J Cell Sci*. 1995;108:1307–1315.
16. Niederöst BP, Zimmermann DR, Schwab ME, Bandtlow CE. Bovine CNS myelin contains neurite growth-inhibitory activity associated with chondroitin sulfate proteoglycans. *J Neurosci*. 1999;19:8979–8989.
17. McKeon RJ, Höke A, Silver J. Injury-induced proteoglycans inhibit the potential for laminin-mediated axon growth on astrocytic scars. *Exp Neurol*. 1995;136:32–43.
18. Fidler PS, Schuette K, Asher RA, et al. Comparing astrocytic cell lines that are inhibitory or permissive for axon growth: the major axon-inhibitory proteoglycan is NG2. *J Neurosci*. 1999;19:8778–8788.
19. Fernaud-Espinosa I, Nieto-Sampedro M, Bovolenta P. Differential effects of glycosaminoglycans on neurite outgrowth from hippocampal and thalamic neurones. *J Cell Sci*. 1994;107:1437–1448.
20. Gilbert RJ, McKeon RJ, Darr A, Calabro A, Hascall VC, Bellamkonda RV. CS-4,6 is differentially upregulated in glial scar and is a potent inhibitor of neurite extension. *Mol Cell Neurosci*. 2005;29:545–558.
21. Ughrin YM, Chen ZJ, Levine JM. Multiple regions of the NG2 proteoglycan inhibit neurite growth and induce growth cone collapse. *J Neurosci*. 2003;23:175–186.

22. Wang H, Katagiri Y, McCann TE, et al. Chondroitin-4-sulfation negatively regulates axonal guidance and growth. *J Cell Sci*. 2008;121:3083–3091.
23. Davies SJ, Fitch MT, Memberg SP, Hall AK, Raisman G, Silver J. Regeneration of adult axons in white matter tracts of the central nervous system. *Nature*. 1997;390:680–683.
24. Bradbury EJ, Moon LD, Popat RJ, et al. Chondroitinase ABC promotes functional recovery after spinal cord injury. *Nature*. 2002;416:636–640.
25. Brittis PA, Canning DR, Silver J. Chondroitin sulfate as a regulator of neuronal patterning in the retina. *Science*. 1992; 255:733–736.
26. Ichijo H, Kawabata I. Roles of the telencephalic cells and their chondroitin sulfate proteoglycans in delimiting an anterior border of the retinal pathway. *J Neurosci*. 2001;21: 9304–9314.
27. Lee H, McKeon RJ, Bellamkonda RV. Sustained delivery of thermostabilized chABC enhances axonal sprouting and functional recovery after spinal cord injury. *Proc Natl Acad Sci U S A*. 2010;107:3340–3345.
28. Moon LD, Asher RA, Rhodes KE, Fawcett JW. Relationship between sprouting axons, proteoglycans and glial cells following unilateral nigrostriatal axotomy in the adult rat. *Neuroscience*. 2002;109:101–117.
29. Walz A, Anderson RB, Irie A, Chien CB, Holt CE. Chondroitin sulfate disrupts axon pathfinding in the optic tract and alters growth cone dynamics. *J Neurobiol*. 2002;53:330–342.
30. Faissner A, Clement A, Lochter A, Streit A, Mandl C, Schachner M. Isolation of a neural chondroitin sulfate proteoglycan with neurite outgrowth promoting properties. *J Cell Biol*. 1994;126:783–799.
31. Clement AM, Nadanaka S, Masayama K, Mandl C, Sugahara K, Faissner A. The DSD-1 carbohydrate epitope depends on sulfation, correlates with chondroitin sulfate D motifs, and is sufficient to promote neurite outgrowth. *J Biol Chem*. 1998; 273:28444–28453.
32. Clement AM, Sugahara K, Faissner A. Chondroitin sulfate E promotes neurite outgrowth of rat embryonic day 18 hippocampal neurons. *Neurosci Lett*. 1999;269:125–128.
33. Jones LL, Sajed D, Tuszynski MH. Axonal regeneration through regions of chondroitin sulfate proteoglycan deposition after spinal cord injury: a balance of permissiveness and inhibition. *J Neurosci*. 2003;23:9276–9288.
34. Bao X, Nishimura S, Mikami T, Yamada S, Itoh N, Sugahara K. Chondroitin sulfate/dermatan sulfate hybrid chains from embryonic pig brain, which contain a higher proportion of L-iduronic acid than those from adult pig brain, exhibit neuritogenic and growth factor binding activities. *J Biol Chem*. 2004;279:9765–9776.
35. Gama CI, Tully SE, Sotogaku N, et al. Sulfation patterns of glycosaminoglycans encode molecular recognition and activity. *Nat Chem Biol*. 2006;2:467–473.
36. Maeda N. Structural variation of chondroitin sulfate and its roles in the central nervous system. *Cent Nerv Syst Agents Med Chem*. 2010;10:22–31.
37. Sugahara K, Mikami T. Chondroitin/dermatan sulfate in the central nervous system. *Curr Opin Struct Biol*. 2007;17:536–545.
38. Snow DM, Brown EM, Letourneau PC. Growth cone behavior in the presence of soluble chondroitin sulfate proteoglycan (CSPG), compared to behavior on CSPG bound to laminin or fibronectin. *Int J Dev Neurosci*. 1996;14:331–349.
39. Zimmer G, Schanuel SM, Bürger S, et al. Chondroitin sulfate acts in concert with semaphorin 3A to guide tangential migration of cortical interneurons in the ventral telencephalon. *Cereb Cortex*. 2010;20:2411–2422.
40. de Wit J, Verhaagen J. Proteoglycans as modulators of axon guidance cue function. *Adv Exp Med Biol*. 2007;600:73–89.
41. Bovolenta P, Fernaud-Espinosa I. Nervous system proteoglycans as modulators of neurite outgrowth. *Prog Neurobiol*. 2000;61:113–132.
42. Snow DM, Steindler DA, Silver J. Molecular and cellular characterization of the glial roof plate of the spinal cord and optic tectum: a possible role for a proteoglycan in the development of an axon barrier. *Dev Biol*. 1990;138:359–376.
43. Seo H, Geisert EE Jr. A keratan sulfate proteoglycan marks the boundaries in the cortical barrel fields of the adult rat. *Neurosci Lett*. 1995;197:13–16.
44. Geisert EE Jr, Bidanset DJ. A central nervous system keratan sulfate proteoglycan: localization to boundaries in the neonatal rat brain. *Brain Res Dev Brain Res*. 1993;75:163–173.
45. Hemming FJ, Saxod R. Keratan sulphate is present in developing chick skin in vivo where it could constitute a barrier to advancing neurites as observed in vitro. *J Neurosci Res*. 1997;48:133–145.
46. Macé K, Saxod R, Feuerstein C, Sadoul R, Hemming FJ. Chondroitin and keratan sulfates have opposing effects on attachment and outgrowth of ventral mesencephalic explants in culture. *J Neurosci Res*. 2002;70:46–56.
47. Ito Z, Sakamoto K, Imagama S, et al. N-acetylglucosamine 6-O-sulfotransferase-1-deficient mice show better functional recovery after spinal cord injury. *J Neurosci*. 2010;30:5937–5947.
48. Cafferty WB, Bradbury EJ, Lidierth M, et al. Chondroitinase ABC-mediated plasticity of spinal sensory function. *J Neurosci*. 2008;28:1998–2009.
49. Li HP, Homma A, Sango K, Kawamura K, Raisman G, Kawano H. Regeneration of nigrostriatal dopaminergic axons by degradation of chondroitin sulfate is accompanied by elimination of the fibrotic scar and glia limitans in the lesion site. *J Neurosci Res*. 2007;85:536–547.
50. Houle JD, Tom VJ, Mayes D, Wagoner G, Phillips N, Silver J. Combining an autologous peripheral nervous system "bridge" and matrix modification by chondroitinase allows robust, functional regeneration beyond a hemisection lesion of the adult rat spinal cord. *J Neurosci*. 2006;26:7405–7415.
51. Curinga GM, Snow DM, Mashburn C, et al. Mammalian-produced chondroitinase AC mitigates axon inhibition by chondroitin sulfate proteoglycans. *J Neurochem*. 2007;102: 275–288.
52. Pizzorusso T, Medini P, Landi S, Baldini S, Berardi N, Maffei L. Structural and functional recovery from early monocular deprivation in adult rats. *Proc Natl Acad Sci U S A*. 2006;103: 8517–8522.
53. Tester NJ, Howland DR. Chondroitinase ABC improves basic and skilled locomotion in spinal cord injured cats. *Exp Neurol*. 2008;209:483–496.
54. Bernhardt RR, Schachner M. Chondroitin sulfates affect the formation of the segmental motor nerves in zebrafish embryos. *Dev Biol*. 2000;221:206–219.
55. Masuda T, Fukamauchi F, Takeda Y, et al. Developmental regulation of notochord-derived repulsion for dorsal root ganglion axons. *Mol Cell Neurosci*. 2004;25:217–227.
56. Golding JP, Tidcombe H, Tsoni S, Gassmann M. Chondroitin sulphate-binding molecules may pattern central projections of sensory axons within the cranial mesenchyme of the developing mouse. *Dev Biol*. 1999;216:85–97.
57. Müller LJ, Marfurt CF, Kruse F, Tervo TMT. Corneal nerves: structure, contents and function. *Exp Eye Res*. 2003;76:521–542.
58. Marfurt CF, Kingsley RE, Echtenkamp SE. Sensory and sympathetic innervation of the mammalian cornea. A retrograde tracing study. *Invest Opbthalmol Vis Sci*. 1989; 30:461–472.

59. Lwigale PY. Embryonic origin of avian corneal sensory nerves. *Dev Biol*. 2001;239:323–337.
60. Bee JA. The development and pattern of innervation of the avian cornea. *Dev Biol*. 1982;92:5–15.
61. Riley NC, Lwigale PY, Conrad GW. Specificity of corneal nerve positions during embryogenesis. *Mol Vis*. 2001;7:297–304.
62. Conrad AH, Strafuss JM, Wittman MD, Conway S, Conrad GW. Thyroxine increases the rate but does not alter the pattern of innervation during embryonic chick corneal development. *Invest Ophthalmol Vis Sci*. 2008;49:139–153.
63. Funderburgh JL, Caterson B, Conrad GW. Keratan sulfate proteoglycan during embryonic development of the chicken cornea. *Dev Biol*. 1986;116:267–277.
64. Hart GW. Biosynthesis of glycosaminoglycans during corneal development. *J Biol Chem*. 1976;251:6513–6521.
65. Takahashi I, Nakamura Y, Hamada Y, Nakazawa K. Immunohistochemical analysis of proteoglycan biosynthesis during early development of the chicken cornea. *J Biochem*. 1999;126:804–814.
66. Young RD, Gealy EC, Liles M, Caterson B, Ralphs JR, Quantock AJ. Keratan sulfate glycosaminoglycan and the association with collagen fibrils in rudimentary lamellae in the developing avian cornea. *Invest Ophthalmol Vis Sci*. 2007;48:3083–3088.
67. Zhang Y, Conrad AH, Tasheva ES, et al. Detection and quantification of sulfated disaccharides from keratan sulfate and chondroitin/dermatan sulfate during chick corneal development by ESI-MS/MS. *Invest Ophthalmol Vis Sci*. 2005;46:1604–1614.
68. Kubilus JK, Linsenmayer TF. Developmental guidance of embryonic corneal innervation: roles of Semaphorin3A and Slit2. *Dev Biol*. 2010;344:172–184.
69. Lwigale PY, Bronner-Fraser M. Lens-derived Semaphorin3A regulates sensory innervation of the cornea. *Dev Biol*. 2007;306:750–759.
70. Dillon TE, Saldanha J, Giger R, Verhaagen J, Rochlin MW. Sema3A regulates the timing of target contact by cranial sensory axons. *J Comp Neurol*. 2004;470:13–24.
71. Keynes R, Tannahill D, Morgenstern DA, Johnson AR, Cook GM, Pini A. Surround repulsion of spinal sensory axons in higher vertebrate embryos. *Neuron*. 1997;18:889–897.
72. Schwend T, Lwigale PY, Conrad GW. Nerve repulsion by the lens and cornea during cornea innervation is dependent on Robo-Slit signaling and diminishes with neuron age. *Dev Biol*. 2012;363:115–127.
73. Suzuki S, Saito H, Yamagata T, et al. Formation of three types of disulfated disaccharides from chondroitin sulfates by chondroitinase digestion. *J Biol Chem*. 1968;243:1543–1550.
74. Zhang Y, Kariya Y, Conrad AH, Tasheva ES, Conrad GW. Analysis of keratan sulfate oligosaccharides by electrospray ionization tandem mass spectrometry. *Anal Chem*. 2005;77:902–910.
75. Alexander JE, Hunt DF, Lee MK, et al. Characterization of posttranslational modifications in neuron-specific class III beta-tubulin by mass spectrometry. *Proc Natl Acad Sci U S A*. 1991;88:4685–4689.
76. Lee MK, Rebhun LI, Frankfurter A. Posttranslational modification of class III beta-tubulin. *Proc Natl Acad Sci U S A*. 1990;87:7195–7199.
77. Lee MK, Tuttle JB, Rebhun LI, Cleveland DW, Frankfurter A. The expression and posttranslational modification of a neuron-specific beta-tubulin isotype during chick embryogenesis. *Cell Motil Cytoskeleton*. 1990;17:118–132.
78. Koo SJ, Clark-Alderfer JD, Tanaka H, et al. Species-specific immunostaining of embryonic corneal nerves: techniques for inactivating endogenous peroxidases and demonstration of lateral diffusion of antibodies in the plane of the corneal stroma. *J Neurosci Methods*. 1998;85:63–71.
79. Avnur Z, Geiger B. Immunocytochemical localization of native chondroitin-sulfate in tissues and cultured cells using specific monoclonal antibody. *Cell*. 1984;38:811–822.
80. Sobue M, Takeuchi J, Fukatsu T, et al. Immunohistochemical techniques for detection of dermatan sulfate proteoglycan in tissue sections. *Stain Technol*. 1989;64:43–47.
81. Funderburgh JL, Stenzel-Johnson PR, Chandler JW. Corneal glycosaminoglycan synthesis in long-term organ culture. *Invest Ophthalmol Vis Sci*. 1983;24:208–213.
82. Caterson B, Griffin J, Mahmoodian F, Sorrell JM. Monoclonal antibodies against chondroitin sulphate isomers: their use as probes for investigating proteoglycan metabolism. *Biochem Soc Trans*. 1990;18:820–823.
83. Caterson B, Mahmoodian F, Sorrell JM, et al. Modulation of native chondroitin sulphate structure in tissue development and in disease. *J Cell Sci*. 1990;97:411–417.
84. Sorrell JM, Mahmoodian F, Schafer IA, Davis B, Caterson B. Identification of monoclonal antibodies that recognize novel epitopes in native chondroitin/dermatan sulfate glycosaminoglycan chains: their use in mapping functionally distinct domains of human skin. *J Histochem Cytochem*. 1990;38:393–402.
85. Caterson B, Christner JE, Baker JR. Identification of a monoclonal antibody that specifically recognizes corneal and skeletal keratan sulfate. Monoclonal antibodies to cartilage proteoglycan. *J Biol Chem*. 1983;258:8848–8854.
86. Petrinovic MM, Duncan CS, Bourikas D, et al. Neuronal Nogo-A regulates neurite fasciculation, branching and extension in the developing nervous system. *Development*. 2010;137:2539–2550.
87. Rutishauser U, Gall WE, Edelman GM. Adhesion among neural cells of the chick embryo. IV. Role of the cell surface molecule CAM in the formation of neurite bundles in cultures of spinal ganglia. *J Cell Biol*. 1978;79:382–393.
88. Meiners S, Mercado ML, Nur-e-Kamal MS, Geller HM. Tenascin-C contains domains that independently regulate neurite outgrowth and neurite guidance. *J Neurosci*. 1999;19:8443–8453.
89. Kubilus JK, Linsenmayer TF. Developmental corneal innervation: interactions between nerves and specialized apical corneal epithelial cells. *Invest Ophthalmol Vis Sci*. 2010;51:782–789.
90. Gibson DA, Ma L. Developmental regulation of axon branching in the vertebrate nervous system. *Development*. 2011;138:183–195.
91. Giger RJ, Hollis ER II, Tuszynski MH. Guidance molecules in axon regeneration. *Cold Spring Harb Perspect Biol*. 2010;2:a001867.
92. O'Donnell M, Chance RK, Bashaw GJ. Axon growth and guidance: receptor regulation and signal transduction. *Annu Rev Neurosci*. 2009;32:383–412.
93. Zhang Y, Yeh J, Richardson PM, Bo X. Cell adhesion molecules of the immunoglobulin superfamily in axonal regeneration and neural repair. *Restor Neurol Neurosci*. 2008;26:81–96.
94. Conrad AH, Zhang Y, Tasheva ES, Conrad GW. Proteomic analysis of potential keratan sulfate, chondroitin sulfate A, and hyaluronic acid molecular interactions. *Invest Ophthalmol Vis Sci*. 2010;51:4500–4515.
95. McKenna CC, Munjaal RP, Lwigale PY. Distinct roles for neuropilin1 and neuropilin2 during mouse corneal innervation. *PLoS One*. 2012;7:e37175.
96. Dutt S, Cassoly E, Dours-Zimmermann MT, Matasci M, Stoeckli ET, Zimmermann DR. Versican V0 and V1 direct the growth of peripheral axons in the developing chick hindlimb. *J Neurosci*. 2011;31:5262–5270.

97. Doane KJ, Ting WH, McLaughlin JS, Birk DE. Spatial and temporal variations in extracellular matrix of periocular and corneal regions during corneal stromal development. *Exp Eye Res*. 1996;62:271–283.
98. Dunlevy JR, Beales MP, Berryhill BL, Cornuet PK, Hassell JR. Expression of the keratan sulfate proteoglycans lumican, keratocan and osteoglycin/mimecan during chick corneal development. *Exp Eye Res*. 2000;70:349–362.
99. Conrad AH, Conrad GW. The keratocan gene is expressed in both ocular and non-ocular tissues during early chick development. *Matrix Biol*. 2003;22:323–337.
100. Properzi F, Carulli D, Asher RA, et al. Chondroitin 6-sulphate synthesis is up-regulated in injured CNS, induced by injury-related cytokines and enhanced in axon-growth inhibitory glia. *Eur J Neurosci*. 2005;21:378–390.
101. Butterfield KC, Conovaloff A, Caplan M, Panitch A. Chondroitin sulfate-binding peptides block chondroitin 6-sulfate inhibition of cortical neurite growth. *Neurosci Lett*. 2010; 478:82–87.
102. Challacombe JF, Snow DM, Letourneau PC. Actin filament bundles are required for microtubule reorientation during growth cone turning to avoid an inhibitory guidance cue. *J Cell Sci*. 1996;109:2031–2040.
103. Challacombe JF, Snow DM, Letourneau PC. Dynamic microtubule ends are required for growth cone turning to avoid an inhibitory guidance cue. *J Neurosci*. 1997;17:3085–3095.
104. Snow DM, Mullins N, Hynds DL. Nervous system-derived chondroitin sulfate proteoglycans regulate growth cone morphology and inhibit neurite outgrowth: a light, epifluorescence, and electron microscopy study. *Microsc Res Tech*. 2001;54:273–286.
105. Kelly TA, Katagiri Y, Vartanian KB, et al. Localized alteration of microtubule polymerization in response to guidance cues. *J Neurosci Res*. 2010;88:3024–3033.
106. Rafuse VF, Landmesser LT. The pattern of avian intramuscular nerve branching is determined by the innervating motoneuron and its level of polysialic acid. *J Neurosci*. 2000;20:1056–1065.
107. Tang J, Landmesser L, Rutishauser U. Polysialic acid influences specific pathfinding by avian motoneurons. *Neuron*. 1992;8:1031–1044.
108. Tang J, Rutishauser U, Landmesser L. Polysialic acid regulates growth cone behavior during sorting of motor axons in the plexus region. *Neuron*. 1994;13:405–414.
109. Landmesser L, Dahm L, Tang JC, Rutishauser U. Polysialic acid as a regulator of intramuscular nerve branching during embryonic development. *Neuron*. 1990;4:655–667.
110. Mao X, Schwend T, Conrad GW. Expression and localization of neural cell adhesion molecule and polysialic acid during chick corneal development. *Invest Ophthalmol Vis Sci*. 2012;53:1234–1243.
111. Qin P, Piechocki M, Lu S, Kurpakus MA. Localization of basement membrane-associated protein isoforms during development of the ocular surface of mouse eye. *Dev Dyn*. 1997;209:367–376.
112. Berardi M, Hindelang C, Felix JM, Stoeckel ME. L1 and laminin: their expression during rat hypophysis ontogenesis and in adult neurohemal areas. *Int J Dev Neurosci*. 1999;17: 121–130.
113. Ohyama K, Kawano H, Asou H, et al. Coordinate expression of L1 and 6B4 proteoglycan/phosphacan is correlated with the migration of mesencephalic dopaminergic neurons in mice. *Brain Res Dev Brain Res*. 1998;107:219–226.
114. Araki K, Ohashi Y, Kinoshita S, Hayashi K, Kuwayama Y, Tano Y. Epithelial wound healing in the denervated cornea. *Curr Eye Res*. 1994;13:203–211.
115. Beuerman RW, Rozsa AJ. Collateral sprouts are replaced by regenerating neurites in the wounded corneal epithelium. *Neurosci Lett*. 1984;44:99–104.
116. Beuerman RW, Schimmelpfennig B. Sensory denervation of the rabbit cornea affects epithelial properties. *Exp Neurol*. 1980;69:196–201.
117. Gilbard JP, Rossi SR. Tear film and ocular surface changes in a rabbit model of neurotrophic keratitis. *Ophthalmology*. 1990;97:308–312.